UNIVERSIDADE DE SÃO PAULO

Escola de Engenharia de São Carlos

Interaction models between humans and lower-limbs exoskeletons applied to robotic neurorehabilitation

Denis Mosconi

Supervisor: Prof. Dr. Adriano Almeida Gonçalves Siqueira

EESC · USP

UNIVERSITY OF SÃO PAULO
SÃO CARLOS SCHOOL OF ENGINEERING

Denis Mosconi

Interaction models between humans and lower-limbs exoskeletons applied to robotic neurorehabilitation

São Carlos

2020

Denis Mosconi

Interaction models between humans and lower-limbs exoskeletons applied to robotic neurorehabilitation

Dissertation presented to the São Carlos School of Engineering of the University of São Paulo, to obtain the title of Master of Science - Graduate Program in Mechanical Engineering.

Concentration area: Dynamics and Mechatronics

Supervisor: Prof. Dr. Adriano Almeida Gonçalves Siqueira

VERSÃO CORRIGIDA

São Carlos

2020

Denis Mosconi
S856m Interaction models between humans and lower-limbs exoskeletons applied to robotic neurorehabilitation / Denis Mosconi ; orientador Adriano Almeida Gonçalves Siqueira. – São Carlos, 2020.
84 p. : il. (algumas color.) ; 30 cm.

Master Dissertation - Graduate Program in Mechanical Engineering and Area of Concentration in Dynamics and Mechatronics – São Carlos School of Engineering, University of São Paulo, 2020.

1. OpenSim. 2. Human-robot interaction. 3. Stroke. 4. Robot-assisted Therapy. I. Siqueira, Adriano Almeida Gonçalves, orient. II. Interaction models between humans and lower-limbs exoskeletons applied to robotic neurorehabilitation.

FOLHA DE JULGAMENTO

Candidato: Tecnólogo **DENIS CÉSAR MOSCONI PEREIRA.**

Título da dissertação: "Modelos de interação entre humanos e exoesqueletos de membros inferiores aplicados em neuroreabilitação robótica".

Data da defesa: 23/03/2020

Comissão Julgadora	**Resultado**
Prof. Associado **Adriano Almeida Gonçalves Siqueira (Orientador)** (Escola de Engenharia de São Carlos/EESC)	APROVADO
Prof. Dr. **Marko Ackerman** (Centro Universitário FEI)	APROVADO
Prof. Dr. **Antônio Padilha Lanari Bó** (Universidade de Brasília/UnB)	APROVADO

Coordenador do Programa de Pós-Graduação em Engenharia Mecânica:
Prof. Associado **Carlos de Marqui Junior**

Presidente da Comissão de Pós-Graduação:
Prof. Titular **Murilo Araujo Romero**

This work is dedicate to all those who have once suffered the consequences of a stroke, either in oneself or in a loved one.

ACKNOWLEDGEMENTS

To God, for He blessed my steps, giving me light for the path and conditions to have conquered the unimaginable.

To my beloved wife Teily, who has always been by my side motivating me. Thank you, my love, for the patience and understanding that you had during the times that I had to be absent to do this work.

To my mother Denise and my father César who have always helped, motivated and often left to achieve things for themselves in order to give me a wonderful life.

To my sisters Luana and Nina, who have always been companions and motivators, giving me courage in times of difficulty.

To my advisor Prof. Dr. Adriano, who taught me not only the wonders of robotic neurorehabilitation, but also how to be a better person.

To my friends Polyana Nunes, Diego Bruno, Alberto Lyra and Fernando del Monte, who helped me a lot in this important phase of my life.

"To move things is all mankind can do, and that for such the sole executant is muscle, whether in whispering a syllable or in felling a forest."

Charles Scott Sherrington

ABSTRACT

MOSCONI, D. **Interaction models between humans and lower-limbs exoskeletons applied to robotic neurorehabilitation**. 2020. 84p. Master Dissertation - São Carlos School of Engineering, University of São Paulo, São Carlos, 2020.

The number of strokes has grown steadily, causing thousands of victims around the world. Approximately 90% of stroke survivors remain with some disability, requiring physical therapy of rehabilitation in order to recover the skills of carrying out the activities of daily living. The use of robots in post-stroke rehabilitation therapies has been shown to be a promising alternative to increase the efficacy of the treatment. The assurance of a human-robot interaction safe for the patient and useful for treatment has been widely studied in the field of rehabilitation engineering, focusing on the development of human-robot interaction controls and biomimetic robots, such as exoskeletons. But the validation and test of this resources is still a challenge: How to do this with reduced cost, low time consumption and without putting patients at risk? The objective of this work was to develop a computational human-exoskeleton interaction model and a forward dynamics-based simulation environment, capable of being applied in the development of interaction controls used in the rehabilitation of lower limbs. The interaction model was developed using computational neuromusculoskeletal systems from OpenSim, with virtual models of the robot actuators coupled to it. The simulation environment was developed in MATLAB, using the OpenSim API. Both the interaction model and the simulation environment were validated using data from physical experiments. Four fully computational simulations were performed with different interaction and movement controls. The results obtained proved that the model and the simulation environment are feasible and useful for the development and simulation of interaction controls between humans and lower limb exoskeletons, saving money, time and ensuring the safety of the user and the equipment used.

Keywords: OpenSim. Human-robot interaction. Stroke. Robot-assisted Therapy.

RESUMO

MOSCONI, D. **Interaction models between humans and lower-limbs exoskeletons applied to robotic neurorehabilitation**. 2020. 84p. Master Dissertation - São Carlos School of Engineering, University of São Paulo, São Carlos, 2020.

O número de ocorrências de AVC tem crescido continuamente, fazendo milhares de vítimas ao redor do mundo. Aproximadamente 90% dos sobreviventes de AVC permanecem com alguma deficiência, necessitando de fisioterapia de reabilitação para recuperar a capacidade de realizar as atividades cotidianas. O uso de robôs em terapias de reabilitação pós AVC tem se mostrado uma alternativa promissora para aumentar a eficácia do tratamento. A garantia de uma interação homem-robô segura para o paciente e útil para o tratamento tem sido amplamente estudada no campo da engenharia de reabilitação, com foco no desenvolvimento de controles de interação homem-robô e robôs biomiméticos, tais como exoesqueletos. Mas a validação e teste desses recursos ainda é um desafio: como fazer isso com custo reduzido, baixo consumo de tempo e sem colocar os pacientes em risco? O objetivo deste trabalho foi desenvolver um modelo computacional de interação humano-exoesqueleto e um ambiente de simulação baseado em dinâmica direta, capazes de serem aplicados no desenvolvimento de controles de interação utilizados na reabilitação de membros inferiores. O modelo de interação foi desenvolvido utilizando sistemas neuromusculoesqueléticos computacionais do OpenSim, com modelos virtuais dos atuadores de robô acoplados a eles. O ambiente de simulação foi desenvolvido no MATLAB utilizando a API do OpenSim. Tanto o modelo de interação quanto o ambiente de simulação foram validados utilizando dados oriundos de experimentos físicos. Quatro simulações totalmente computacionais foram realizadas com diferentes controles de interação e movimentos. Os resultados obtidos provaram que o modelo e o ambiente de simulação são factíveis e úteis para o desenvolvimento e simulação de controles de interação entre humanos e exoequeletos de membros inferiores, poupando dinheiro, tempo e garantindo a segurança do usuário e do equipamento utilizado.

Palavras-chave: OpenSim. Interação Humano-robô. Acidente Vascular Cerebral. Terapia assistida por robô.

LIST OF FIGURES

LIST OF TABLES

LIST OF ABBREVIATIONS AND ACRONYMS

ADL	Activities of Daily Living
AVC	Acidente Vascular Cerebral
API	Application Programming Interface
CPG	Central Pattern Generator
CNS	Central Nervous System
EMG	Electromyography
FES	Functional Electrical Stimulation
GRF	Ground Reaction Forces
HNP	Hybrid Neuroprosthesis
NMS	Neuromusculoskeletal system
TIA	Transient Ischemic Attack

LIST OF SYMBOLS

θ^d	Desired position of the joint
$\hat{\theta}$	Real position of the joint obtained with simulation
θ_e	Position error
τ_R	Torque developed by the exoskeleton
τ_{FF}	Torque developed by the user, from the forward loop and based on the internal model
τ_{PID}	Torque developed by the user, from the feedback loop and based on the tracking errors
τ_{Total}	Sum of robot and user torques.
τ_{optm}	Maximum torque applied by the virtual exoskeleton actuators

CONTENTS

1 INTRODUCTION

Stroke is a noncommunicable disease of the cardiovascular type, caused by the suspension of the blood supply to the brain because a bleeding (hemorrhagic stroke) or a clot (ischemic stroke). In the last 15 years, the disease was the second leading cause of death in the world. Annually, about 15 million people worldwide suffer a stroke (every two seconds someone in the world has a stroke). Of these, 5 million die and another 5 million remain permanently disabled (MACKAY; MENSAH, 2004; WHO, 2011b; WHO, 2018).

If you took a minute to read the previous paragraph, 30 people around the world suffered a stroke at this time and 10 of them now have some permanent motor impairment. For these people, tasks that were simple and common a minute ago, such as button a shirt, brush the hair, writing, eating and walking, now are a great challenge or even impossible to be executed without the help of someone.

According to the Brazilian Ministry of Health, 10% of the deaths in the country are caused by stroke, and in 2016 there were 188,223 hospitalizations and 40,019 deaths caused by the disease (MS, 2018b).

The World Health Organization forecasts a continuous increase in stroke occurrences. Some factors help explain this upward trend: sedentary lifestyle, incorrect diet, alcohol, tobacco and population aging. It is expected that by 2030 there will be approximately 200 million people with some motor disability due to stroke, which is approximately the number of the current Brazilian population (WHO, 2011b).

Approximately 90% of stroke survivors remain with some disability (HOGAN, 2014). The severity and localization of the stroke in the brain determines the type and severity of the disability. Some examples of disabilities are are the difficulty of speaking and understanding, vision problems and weakness in arms and legs, increasing the patient dependency on others to execute activities of daily living (ADL) such as walking, dressing, writing and eating.

The way the blood is transported to the brain makes the most rostral parts the more susceptible to blockage. This rostral areas of the Central Nervous System (CNS) are the cerebral hemispheres, which include areas of the cerebral cortex that are responsible for sensory-motor coordination (HOGAN, 2014). Then, to recover the motor capabilities of a stroke survivor (e.g. gait pattern, equilibrium), physical therapy involving rehabilitation makes necessary.

The therapy of rehabilitation consists in the execution of specific movements in order to provoke motor plasticity to the patient, improving motor recovery, minimizing functional deficits and helping the subject to be reinserted into social life (DIAZ; GIL;

SANCHEZ, 2011).

The neuroplasticity consists in a reorganization of the functional areas of the cerebral cortex, allowing the brain to move motor centers to other areas not affected by the stroke, recovering the lost motor function (IBARRA, 2014). To provoke neuroplasticity, very intensive rehabilitation therapies are needed, especially for gait rehabilitation where more than three therapists are often required to manually assist the torso and legs of the patient. This is an exhausting and limited work for both the patient and the therapist and involves high costs to any country's health care system (DIAZ; GIL; SANCHEZ, 2011).

The robotic-assisted therapy is a proponent area to development of rehabilitation activities. Robotic rehabilitation can replace the physical effort of the therapist, ensuring more intensive and repetitive movements, with uniformity, for long-time routines, reliable storage of data regarding the patient, allowing the therapist to quantitatively verify the evolution of the treatment. In addition, rehabilitation robots are able to meet the *Assist-as-Needed Paradigm*, that is to assist the patient to perform the movement in therapy only when necessary, assuming a transparent behavior when the subject can perform the task on its own, contributing to cortical reorganization through neuroplasticity (JUTINICO et al., 2017; DIAZ; GIL; SANCHEZ, 2011).

The interaction between humans and robots is a challenge in the field of robotic rehabilitation, since such interaction should ensure the safety of the patient, meet the therapy requirements for each specific subject and satisfy the assist-as-needed paradigm, predicting the intention of movement of the user. Several interaction controls have been studied in order to reduce the risks and ensure the treatment efficacy: EMG-driven adaptive impedance control (PEÑA, 2017), control strategy based on kinetic motor primitives (NUNES; SANTOS; SIQUEIRA, 2018), performance-based adaptive assistance controller (BAYON et al., 2018), motor intention decoding algorithm (PASTORE et al., 2018), Markovian robust compliance control (JUTINICO et al., 2018), impedance control using functional electrical stimulation (KIM; KIM, 2018).

But the validation and testing of these controllers is still a challenge, as the tests involved demand physical contact between a user and a robot, which can put them at risk of an accident, in addition to demanding time and resources in the preparation of such tests. Then, how to do this with reduced cost, low time consumption and without putting patients at risk? A possible solution is the use of interaction models: Computational models of the human-robot set, attending both the patient's characteristics and the rehabilitation robot, and able to provide reliable data on the interaction controls developed. Such interaction models allow the interaction controls used in robotic rehabilitation to be developed, adjusted and tested, minimizing the need for physical tests involving a user and a robot, which reduces the risk of accidents in addition to saving design time.

1.1 Objectives

The general objective of this work is to develop a patient-exoskeleton interaction model that can be used for validation and testing of interaction controls applied in robotic rehabilitation of lower-limbs.

The specifics objectives are:

- development of a human-exoskeleton interaction model based on a computational model of the human neuromusculoskeletal system coupled to a computational model of a lower-limbs exoskeleton;
- development of an environment for simulation of the controllers applied to the interaction model;
- validation of the interaction model;
- test some interaction controls using the proposed model and simulation environment.

1.2 Dissertation Outline

In Chapter 2 we present the theoretical concepts related to the human movement process and the biomechanism involved. An introduction to the concept of the human internal model is presented. A review on the types of stroke is performed. Methods to rehabilitation of the motor skills are discussed, from the conventional rehabilitation process to robotic neurorehabilitation. The chapter is finalized presenting the human-robot interaction models concept, with a comprehensive review of works related to this theme.

In Chapter 3 are described in detail the tools and methods used in this work. The development of the interaction model is presented, along with the simulation algorithm based on forward dynamics. The method to validate the model and the simulation program is introduced and the interaction controls tested are mentioned.

In Chapter 4 the results obtained through the development and use of the model and the simulation environment are presented and discussed. Here the interaction controls tested are presented in detail, along with the results obtained by simulating such controls.

Chapter 5 presents the conclusions of the results obtained and analyzes carried out. They are also presented the opportunities that this work brings, along with advantages and disadvantages of using interaction models. Suggestions for future work close this chapter.

1.3 Published Works

This section shows the articles published by the author of this dissertation, in journals and congresses.

MOSCONI, Denis; NUNES, Polyana Ferreira; SIQUEIRA, Adriano Almeida Gonçalves. Modeling and control of an active knee orthosis using a computational model of the musculoskeletal system. **Journal of Mechatronics Engineering**, [S.l.], v. 1, n. 3, p. 12 - 19, dec. 2018. ISSN 2595-3230. Doi: https://doi.org/10.21439/jme.v1i3.19.

MOSCONI, Denis; NUNES, Polyana Ferreira; SIQUEIRA, Adriano Almeida Gonçalves. Human-exoskeleton computational model: an approach to the human-machine interaction problem in robotic assisted therapy. In: IV Simpósio do Programa de Pós-Graduação em Engenharia Mecânica da EESC-USP, 2019, São Carlos. **Proceedings...** São Carlos: USP, 2019.

MOSCONI, Denis; NUNES, Polyana Ferreira; PEÑA, Guido Gomez; SIQUEIRA, Adriano Almeida Gonçalves. Human-exoskeleton interaction model applied to robotic neurorehabilitation of lower limbs. In: 25th ABCM International Congress of Mechanical Engineering, 2019, Uberlândia. **Proceedings...** Uberlândia: ABCM, 2019.

MOSCONI, Denis; NUNES, Polyana Ferreira; SIQUEIRA, Adriano Almeida Gonçalves. Feasibility study of human-exoskeleton computer model to simulate interaction controls for robotic assisted rehabilitation. In: X Congreso Iberoamericano de Tecnologías de Apoyo a la Discapacidad, 2019, Buenos Aires. **Proceedings...** Buenos Aires: Aitadis, 2019.

NUNES, Polyana Ferreira; MOSCONI, Denis; SIQUEIRA, Adriano Almeida Gonçalves. Control Design Inspired by Primitive Motors to Coordinate the Functioning of an Active Knee Orthosis for Robotic Rehabilitation. In: X Congreso Iberoamericano de Tecnologías de Apoyo a la Discapacidad, 2019, Buenos Aires. **Proceedings...** Buenos Aires: Aitadis, 2019.

MOSCONI, Denis; SIQUEIRA, Adriano Almeida Gonçalves. Simulation of impedance based interaction control for robotic neurorehabilitation using a human-exoskeleton interaction model inspired by the human internal model. In: XIV Conferência Brasileira de Dinâmica, Controle e Aplicações, 2019, São Carlos. **Proceedings...** São Carlos: USP, 2019.

MOSCONI, Denis; NUNES, Polyana Ferreira; SIQUEIRA, Adriano Almeida Gonçalves. Modelagem e Simulação em Neuroreabilitação Robótica. In: I Mostra de Pesquisa e Extensão do IFSP - Catanduva, 2018, Catanduva. **Proceedings...** Catanduva: IFSP, 2018.

2 THEORETICAL FOUNDATION

This chapter seeks to provide a brief revision about the biomechanics of the human movement, stroke and the rehabilitation of their victims, it also introduces the concept of human-robot interaction models.

The purpose of writing this chapter was to allow people outside the area to become familiar with the context, so if you are familiar with this topic, feel free to skip to the next chapter. However, the author still advises that at least a brief reading of the sections 2.2 and 2.5 be done, as they deal with issues that are crucial for understanding the development of this work.

2.1 Neural Control and Biomechanics of the Human Movement

The system of human motion can be divided into three basic levels: the level of activation of movement (on-off), coordinated by the brain, which determines the beginning and end of motion; the generation of a motion pattern (e.g. coordinated movement of the legs), determined by a group of neurons located in the spinal cord; and the execution of the movement, result of the force exerted by the muscles and tendons on the involved members (Fig. 1) (HALL, 2017; KIRTLEY, 2006).

Figure 1 – Signal flow for locomotion control.

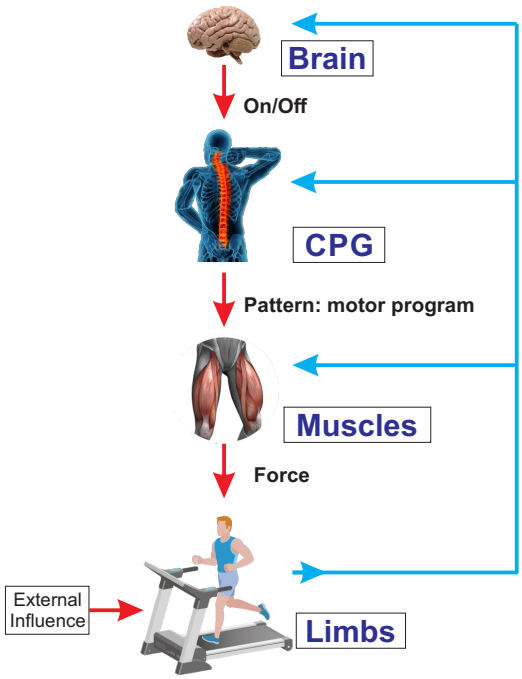

Source: Image generated by the author.

Detailed divisions and interconnections of these basic systems can be realized for a deeper understanding of the process of human locomotion, but it is beyond the scope of this book. In this section the basic functions of the aforementioned levels will be presented in order to provide the reader with a theoretical basis on the human gait. To obtain more in depth information, specific literature should be consulted.

2.1.1 Motor Functions of the Brain

Voluntary movements are initiated when the cerebral motor cortex activates the motor patterns stored in the lower brain areas (e.g. spinal cord). These lower areas, in turn, send the control signals to the involved skeletal muscles, according to the required pattern. The motor cortex is divided into three subareas, each one with specific motor functions: *primary motor cortex, premotor area* and *supplementary motor area* (Fig. 2) (HALL, 2017).

The **primary motor cortex (MI)** contains a map of the muscular system of the body, having a direct functional relationship with the muscles and being responsible for executing movements with normal patterns of complexity. The largest area of the cortex is related to control of hands and lips (SINGH, 2018; HALL, 2017).

Figure 2 – Functional areas of the cerebral cortex.

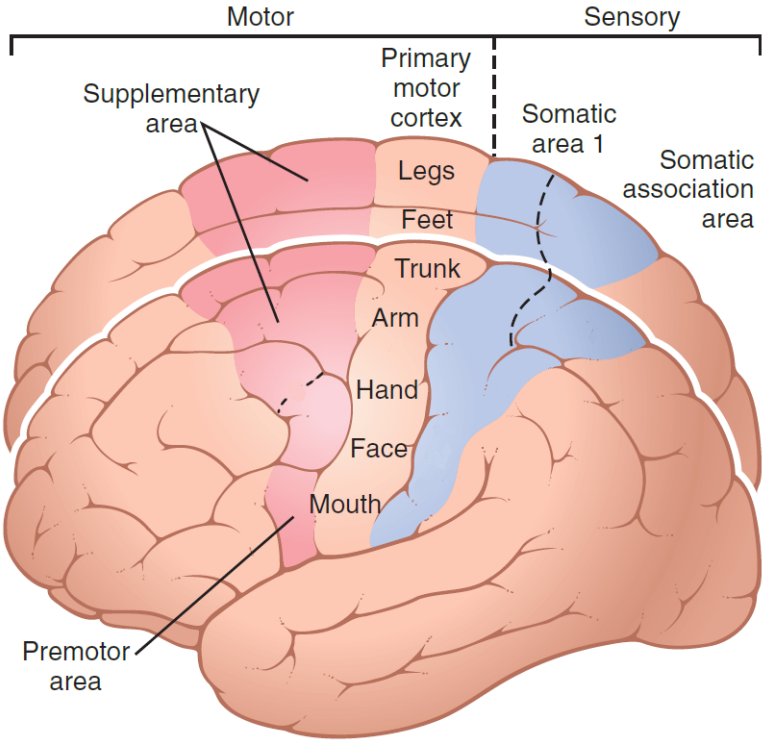

Source: Adapted from (HALL, 2017).

The **premotor area** is responsible for the generation of more complex patterns of movements, than those produced by the primary cortex. In addition, the premotor cortex is responsible for programming the intended movements and to control the movements in execution (SINGH, 2018; HALL, 2017).

The **supplementary motor area (MII)** is responsible for bilateral parallel movements, such as picking up with both hands. This area works in conjunction with the premotor area to generate movements responsible by the body posture, as a basis for finer limb control (HALL, 2017).

Another important part of the brain for motor control is the brain stem, which is composed of the medulla, pons and midbrain (or mesencephalon) (Fig. 3). It can be considered as an extension of the spinal cord into the cranium and is the principal way station for command signals from the higher neural centers. Some of its main functions are maintenance of axial tone of the body for standing and maintenance of the body equilibrium (HALL, 2017).

In addition to the cortical regions of the brain, two other structures essential for controlling movement are the *cerebellum* and the *basal ganglia*. These structures always work in conjunction with other systems of motor control because they are not capable of to control muscle function by itself (HALL, 2017).

Figure 3 – The neural motor system.

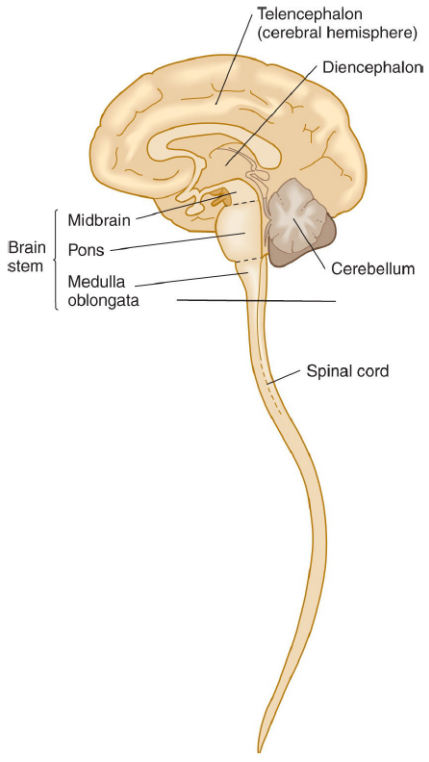

Source: Adapted from (SINGH, 2018).

The cerebellum helps sequence the motor activities and in fast, soft progression from one muscle movement to the next. In addition, it monitors and correctively adjusts body motor activities during its execution, so that they are in accordance with the motor program. The cerebellum also aids the cerebral cortex to plan the next sequential movement while the current movement is still in execution (HALL, 2017).

The basal ganglia assists in the planning and control of complex pattern movements, controlling the relative intensities and directions of the separate movements, and the sequencing of multiple successive and parallel movements in order to achieve specific and complex motor objectives (HALL, 2017).

2.1.2 Central Pattern Generator - CPG

In the spinal level, movement patterns for all muscle areas of the body are programmed. All these programs of the cord can be triggered by higher levels of motor control, or inhibited while the high levels take over the control (HALL, 2017). The human locomotion pattern, that is, the gait function, is centrally generated in the spinal cord, by the *Central Pattern Generator* (CPG) (WYART, 2018).

A Central Pattern Generator is a ensemble of neurons that work together to generate a motor program: a time and target oriented output of the CPG which serves as command to muscles. When muscles receive the CPG commands, they contract and relax in a coordinated sequence, constituting the motor pattern, this is important to ensure the alternating motion of the legs since there is no mechanical coupling between the lower-limbs. (BALABAN et al., 2015; KIRTLEY, 2006).

Descending commands from the brain trigger the Central Pattern Generator to initiate and stop locomotion (Fig. 1). Afferent feedback promotes adaptation of the pattern to the needs of the individual in relation to the environment and the context involved (KIRTLEY, 2006).

Experiments showed that patients who have lost the connections between the motor centers of the brain and the CPG are unable to walk, but, when tonic stimulation was applied to the distal part of the spinal cord, the patients started to walk.(BALABAN et al., 2015).

2.1.3 Muscles: Force Actuators

Together with the bones, the skeletal muscles confer structure and capacity of motion to the body. About 40-45% of the body weight is composed of skeletal muscles, which are attached to the bones via tendons. Such muscles are responsible for all body motion and locomotion, and are normally under voluntary control (ETHIER; SIMMONS, 2017).

The muscles are attached to the bones through a fibrous tissue called tendon. The proximal connection point of the muscles to the bone is the origin and the distal point is the insertion. To perform a movement, the muscles vary their length through the muscular contraction process, and this variation, applied to the insertion point, gives rise to several types of lever whose features depend of the muscle insertion, the position of the fulcrum and the lever, and the length of the lever arm (HALL, 2017).

The muscles are constituted of long multinucleated rod-shaped fibers grouped in *fasciculus* (up to 30 cm in length) (Fig. 4). All these structures are covered by connective tissue: the *epimysium* covers the muscle, the *perimysium* overlies each fasciculus and the *endomysium* covers the muscle fibers. The tissue isolates one structure from the other allowing them to move individually with each other, maintaining the position and directing the displacement (HALL, 2017; ETHIER; SIMMONS, 2017).

Each muscle fiber is composed of *myofibril*, that are long rod-shaped elements responsible for causing the muscle contraction. In turn, the myofibrils are composed of a regular banded structure, whose the repeat unit is called *sarcomere*.

Figure 4 – The skeletal muscle structure. A-muscle, B-muscle fasciculus, C-muscle fiber, D-Myofibril, E-Sarcomere.

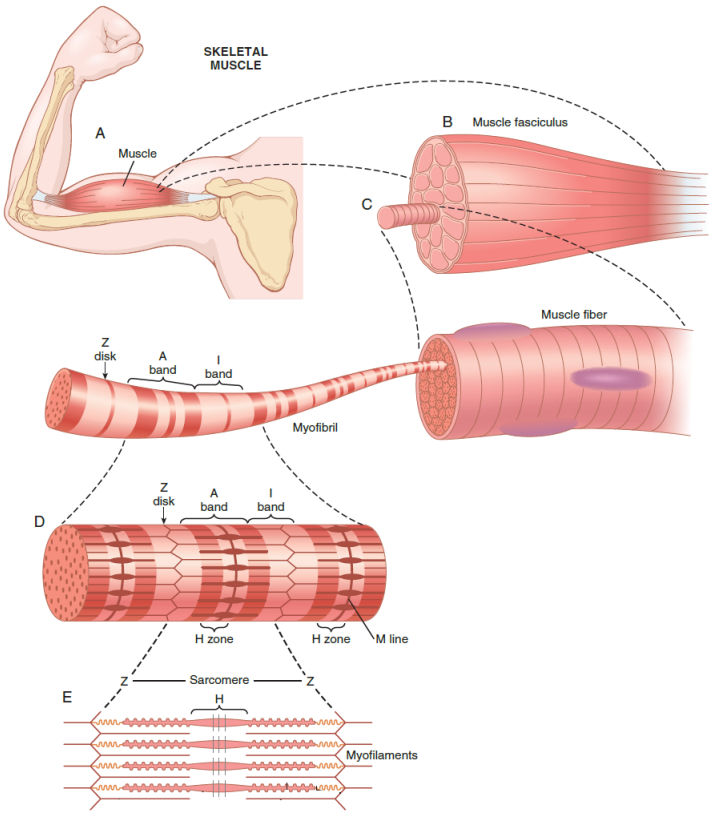

Source: Adapted from (HALL, 2017).

The sarcomere consists of approximately 1500 thick filaments of myosin and 3000 thin filaments of actin. These filaments are arranged as shown in the Figure 5. The Z-line separates one sarcomere from another laterally arranged. The manner myosin and actin are organized gives rise to bands: band A is the portion of the sarcomere where the myosin filaments are found and the band I is the region containing the actin filaments (HALL, 2017).

Figure 5 – The Structure of the sarcomere.

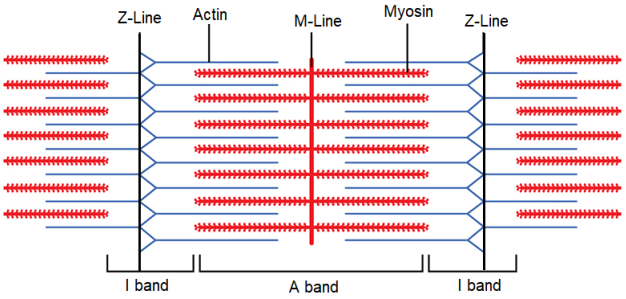

Source: Adapted from (ETHIER; SIMMONS, 2017).

When the muscle activation occurs, a biochemical process causes the actin filaments to slide over the myosin filaments, increasing the region of superposition. As the actin filaments are connected to the z-lines, the increase in the superposition reduces the distance between the z-lines, resulting in the muscle contraction. When activation stops, the biochemical process that caused filament displacement is decremented and the muscle returns to the resting point.

Figure 6 – Active and passive forces of the muscle.

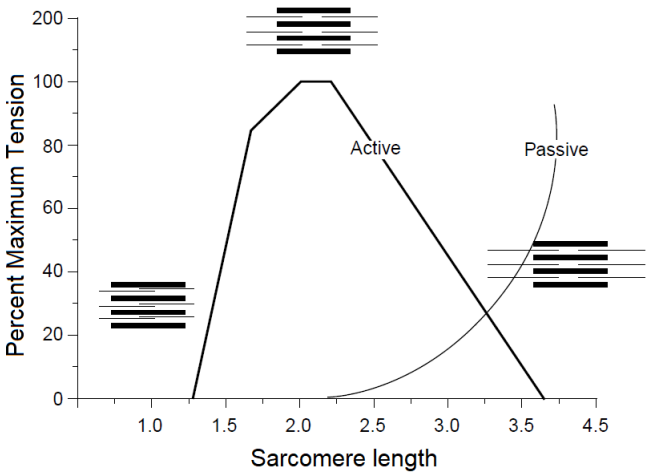

Source: Adapted from (PETERSON; BRONZINO, 2008).

The distance between the Z-lines is directly related to the muscle's ability to produce force. As the actin superposition on myosin increases, the force generated by the muscle increases until the distance between the Z-lines reaches their limit. Thereafter, the ability of the muscle to produce reduces again. When the muscle is stretched to a length above normal the other structures present (connective tissue, nerves, vessels) add a passive force, however, the active force generated during muscle contraction decreases, as shown in Figure 6 (HALL, 2017).

2.2 The Human Internal Model Concept

For a healthy person, the gait movement seems simple and intuitive. However, the neurological and mechanical properties of the motor system introduce a very high level of complexity in this task.

The act of taking a step can be subdivided into some subtasks: destination identification, trajectory planning, motor control signal production, muscle activation and movement execution. To this is added the corrections of deviation from the trajectory due to disturbances that occurred during the execution of the movement.

Precisely how the nervous system selects particular combinations of joints and muscles, as well as determining the production of motor commands, remains not well clear. An approach about the generation of motor commands affirms that these commands are generated through a feedforward-feedback control system as depicted in Figure 1 ((FREY et al., 2011)).

Figure 7 – Feedforward-feedback motor control. The feedback motor command, in addition to eliminating the influence of disturbances and noise, also helps to improve the internal model.

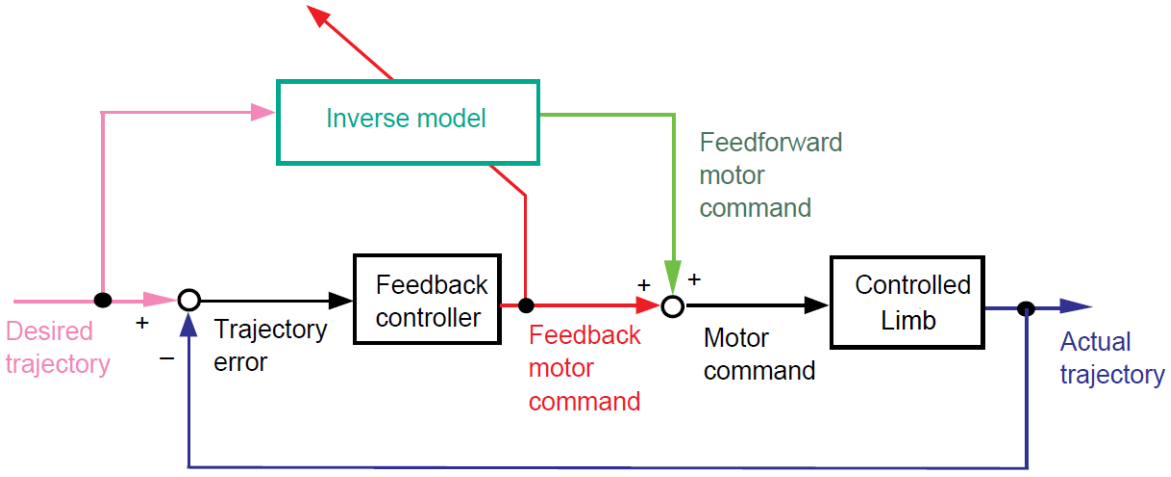

Source: Adapted from (WOLPERT; MIALL; KAWATO, 1998).

In the **Feedforward Control Loop**, given the desired motor action (e.g. move the legs to walking), and the current state of the limbs and environment, an inverse internal model of the human body computes the command to be sent to the muscles. The inverse internal model is a inverse dynamic model of the limbs, located in the cerebellum and able to predict the muscle activations that will produce the torques and forces needed to perform a given movement ((WOLPERT; MIALL; KAWATO, 1998)).

Because there is no need to wait for sensory information, feedforward control does not suffer from the delay problem. However, a purely feedforward controlled system require three essential conditions: a perfect internal model, a static environment and the absence of noise and disturbances in the motor command. As these conditions are impossible to be achieved in the real world, a feedback control loop works together the feedforward control seeking to eliminate any unwanted effects that may compromise the smooth execution of the movement.

In the **Feedback Control Loop** afferent signals that carry information about the error between the desired motion and the performed one are used to generate a correction motor command. In addition, such errors are used to improve the internal model, making the individual gain skill in performing a certain task ((LAM; ANDERSCHITZ; DIETZ, 2006)). Although this control eliminates the influence of disturbances, it is limited by delays in sensory and motor routes, which in the biological nervous system can last a few hundred milliseconds. Thus, a biological control system based purely on a feedback loop is impossible, as it would present large oscillations, which is obviously undesirable in the execution of movements, this reinforces the importance of having a feedforward-feedback control.

In this work, the feedforward-feedback control and human internal model concepts were used to develop the algorithm that reproduces the human behavior.

2.3 Stroke

Stroke (or brain attack) is a cardiovascular noncommunicable disease, characterized by lack of cerebral oxygenation due to an interruption of blood flow to the brain. The first term for stroke (not longer in use) was "*apoplexy*", which in Greek meant "to strike suddenly with violence". The word *stroke* is a reference to being suddenly stricken (CAPLAN, 2005).

The consequences of a stroke appear quickly: less than a minute after the brain has its blood supply interrupted. Most often, stroke is not accompanied by pain, but other symptoms such as inability to speak, paralyzed arms and legs or loss of consciousness. This means that most victims do not understand that they are suffering from a stroke, which can result in greater negative impacts, since the longer it takes to fight a stroke, the more damage can be accumulated.

Stroke implies a high risk of death, being the second leading cause of death around the world. Moreover, the disease causes longer disability than any other medical condition. Survivors may experience some permanent disabilities, such as loss of vision or ability to speak, paralysis or dementia. After a first stroke, within five years, the risk of a recurrent stroke is between 30% and 43% (CAPLAN, 2005; AL., 2004).

Some causes of stroke are: high blood pressure, high cholesterol, obesity, diabetes, tobacco, physical inactivity, alcohol and unhealthy diet (WHO, 2011a). Certain socioeconomic , ethnic, and racial groups also have an increased risk of stroke(MACKAY; MENSAH, 2004). Although strokes be more common in people over 65, it can be occur at any age including infancy, childhood, adolescence, and early adulthood (CAPLAN, 2005).

There are various types of existing stroke that can be classified into three broad groups: *ischemic stroke*, *hemorrhagic stroke* and *transient stroke*.

2.3.1 Ischemic Stroke

This is the most common type of stroke, occurring in 80% of the cases (RUDD; IRWIN; PENHALE, 2004).It occurs when a blood clot forms, blocking the blood flow to a part of the brain, resulting in a painless loss of some brain function (Fig. 8). Most of victims remains with some disability that impacts their lives, requiring rehabilitation treatment. The characteristic signs are weakness of an arm, deformation on one side of the face and inability to speak, to understand language or to walk (MARLER, 2005).

Figure 8 – Ischemic stroke.

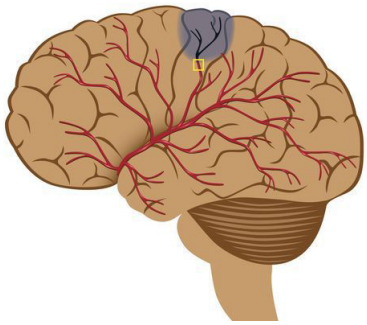

Source: Adapted from (MS, 2018a).

2.3.2 Hemorrhagic Stroke

The hemorrhagic stroke is characterized by a bleeding caused by broken blood vessels, and represents 20% of cases (Fig. 9). The stroke can occur within the brain - *intracerebral hemorrhage* (ICH) - or onto the areas surrounding the brain - *subarachnoid hemorrhage* (SAH) (RUDD; IRWIN; PENHALE, 2004). It is the most dangerous of all types of stroke (MACKAY; MENSAH, 2004).

Brain hemorrhage has the same symptoms of the ischemic stroke, however it becomes worse as the time pass, eventually progressing to coma. In addition, hemorrhagic stroke is more often fatal and cause more severe disability than the ischemic stroke: the probability of a victim to die in the first few days after a brain hemorrhage is 40% (MARLER, 2005).

Figure 9 – Hemorrhagic stroke.

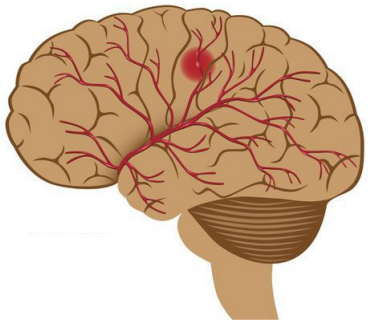

Source: Adapted from (MS, 2018a).

2.3.3 Transient Ischemic Attack (TIA)

It is the same as a ischemic stroke with short duration: the blood flow is decreased temporary to a part of the brain. These attacks are caused by temporary blockage of an artery and its symptoms is related to the region where the stroke occurs.

The duration of a TIA is between two and seven minutes and the patient recovery occurs in approximately 24 hours. These temporary strokes is a warns about something wrong with the body and a more severe stroke can occurs within 24 to 48 hours after (CAPLAN, 2005; MARLER, 2005; RUDD; IRWIN; PENHALE, 2004).

2.4 Recovering the Motor Functions Lost After a Stroke

The most important aspect of a stroke are the consequences in the life of the victim: the loss of function is often instantaneous and totally unanticipated. The loss of brain function makes individuals dependent on others to realize the activities of daily live, what can be dehumanizing (CAPLAN, 2005).

In order to recover lost functions, such as walking ability, patients undergo rehabilitation therapy. About 50 percent of stroke victims need some kind of rehabilitation. Rehabilitation should help to empower a subject with some disability and his or her family (WHO, 2011b; MARLER, 2005).

2.4.1 Rehabilitation

According to de World Health Organization (WHO, 2011b, p. 96), rehabilitation is "a set of measures that assist individuals who experience, or are likely to experience, disability to achieve and maintain optimal functioning in interaction with their environments".

In conventional treatment, the physical therapist uses exercises, training and physical manipulation in order to help the stroke patient to recover the movements, coordination and balance. With the physical therapy, the patient relearn simple motor activities, such as sitting, standing and walking. A wide range of therapies are available and the therapeutic plan with the type of stroke therapy that a victim should receive depends upon of the stage and severity of the disease (PARKER; PARKER, 2002).

Some resources that the physical therapists have to help improve motor control (AL., 2004), are:

- *Biofeedback*: Utilizing electromyography (EMG) as biofeedback, it is possible to determine patient's performance in the course of treatment;
- *Functional Electrical Stimulation (FES)*: It is used to directly stimulate the muscles and peripheral nerves in order to cause movement. This method both improves functionality and increases strength of the muscles.
- *Treadmill Training*: To train walking, the patient has the body supported by a overhead support system, while walking over a treadmill. This is one of the most traditional training of rehabilitation of gait.
- *Robot-assisted Therapy*: A robotic system help the patients to develop a movement, applying force to the affected limb when necessary. The robot can operate in passive or active modes, enabling the subject to repetitively practice movements and giving visual and auditory feedback during the therapy.

2.4.2 Neurorehabilitation

While the word "rehabilitation" is related with recovery of physical skills, the neurorehabilitation can be defined as a "set of methods that aims to restore neurological function lost or impaired due to brain injury", that is, the neurorehabilitation not only recovers the physical abilities, but also the cognitive capacities that command them (MURIE-FERNáNDEZ et al., 2010, p.191). Perhaps, the correct word in the context of the present work is "neurorehabilitation", but here, no difference will be made between it and "rehabilitation".

In order to improve the neurological and functional deficits, the therapists uses advantages of the brain plasticity (MURIE-FERNáNDEZ et al., 2010). "Neuroplasticity

is the ability of neurons and neuron aggregates to adjust their activity and even their morphology to alterations in their environment or patterns of use" (SELZER et al., 2006), that is, the central nervous system has a potential for recovery and adaptation, which can be promoted (BRAININ; HEISS, 2009).

To recover the lost motor skills, the patient must behave actively during the therapy, intending and trying by itself to perform the movements of the therapeutic activities. Passive movements only help to improve the joint mobility, but not motor cognitive ability, so the physiotherapist should support the patient, not perform the exercise for him ou her.

2.4.3 Robotic Neurorehabilitation

The robotic neurorehabilitation combines the features of the robot-assisted therapy with the concepts of neurorehabilitation. During the treatment sections, the therapist relies on the help of robotic systems to assist the patient in the execution of the desired movements, always attending to the assist-as-needed paradigm: the patient should try to perform the movement, and the robot should only aid if he or she can not execute it completely, having its mechanical stiffness adjusted to the characteristics and needs of the patient.

The advantages of the robotic neurorehabilitation is its potential of provide a more repetitive and intensive treatment, with less effort and without overload for therapists; new evaluation methods; and even new manners of interventions enabling the robot for provide repetitive, secure and precisely controllable movements. Robots can to assist in perform a much larger amount of activities of daily living than is currently possible, such as walking and manipulation tasks, increasing the independence and quality of life for the patient (PONS; TORRICELLI, 2014). Robots may also offer the opportunity for therapeutic intervention to more individuals, through the reduction of the quota of therapists needed to attend a single patient (DIETZ; NEF; RYMER, 2012).

According to Lum et al. (2002), the robotic devices can continuously and precisely support and assist the repetitive and stereotyped movements in severely impaired subjects, potentially improving the quality of rehabilitative treatment after stroke.

Krebs et al. (2003) state that a transformation of rehabilitation clinics can be provided by robotics and information technology, evolving the operations from labor-intensive to technology assisted. In addition to being more efficient in delivery certain routine physical and occupational therapy activities, robot-aids also provide a large stream of data that can help patient diagnosis, customization of therapy and maintenance of patient registry.

Robotic devices are a possible way to precisely control and measure therapy, solving the difficulties of quantify dose, type and consistency of rehabilitation activities,

besides to provide new tool for therapists and improve access to therapy for patients (REINKENSMEYER; EMKEN; CRAMER, 2004).

The traditional gait training in rehabilitation therapy is labor-intensive and, therefore, training duration is usually limited by personnel shortage and fatigue of the therapist, not by that of the patient. The ergonomically unfavorable seating posture of the therapist during the treatment causes back pain, culminating in training sessions shorter than may be required to achieve an optimal therapeutic outcome. With robot-assisted gait training, the duration and number of sessions can be increased, while reducing the number of therapists required per patient (RIENER et al., 2005).

A typical session of human administered therapy involves about eighty movements, while a typical session of robot-aided therapy involves over a thousand, which provides the necessary stimulus to the brain to re-acquire movement control and coordination. The active participation of the patient is essential: "passively moving a patient's limbs may help improve joint mobility but it yields no improvement of motor function" (HOGAN, 2014).

In robotic neurorehabilitation, a widely used robotic device is the exoskeleton, whose kinematic is determined according to the human body anatomy, and have more intense physical and cognitive interactions with the user. Exoskeleton can be defined as "structures of rigid links, mounted on the body of some living vertebrae and following the main directions and having the main joints of the living organism's endoskeleton" (VUKOBRATOVIC et al., 1990).

2.5 Human-Robot Interaction Models

Human-Robot Interaction Models can be defined as mathematical-computational objects that are able to simulate, in an computational specific environment, the kinematics and dynamics relationship between a human being and a robot (in this case a exoskeleton of the lower limbs). Through this approach, the human behavior and the robot control can be modeled allowing the rehabilitation engineer and the physiotherapist to develop new ways to rehabilitate the patient efficiently and safety.

Interaction models can be used to develop, test, validate and tunning interaction controls applied to neurorehabilitation. They are able to provide data about the design of robot and their influences in the patients, allowing the researchers to found the best project and parameters for the manufacture of orthosis and rehabilitation robots.

There are many advantages to using interaction models, such as saving time, saving money, and avoiding putting both the user and the equipment at risk. In addition, changes can be made to both the control system and the model quickly compared to physical models.

Some disadvantages are the fact that models are mathematical and computational representations of reality, often having uncertainties that cannot be overlooked in robot and controller designs. In addition, the more complex the model and control, the higher the computational cost.

However, the computational approach in developing tools for robotic neurorehabilitation is a promising tool that will be long-lived, as it allows that controls based on artificial intelligence, modern, robust and optimal control theory to be well designed with time savings, cost reduction and reduced risks.

2.5.1 Related Works

Following are some works that made use of interaction models, either for the development and simulation of interaction controls, biomechanical data acquisition, or even to assist in the development of rehabilitation robots.

An interaction model and an simulation environment were developed by (SOUSA; FREIRE; BO, 2019) to design and comparison of hybrid neuroprosthesis (HNP) controllers for low speeds in rehabilitation. The interaction model was developed from a musculoskeletal model called *leg6dof9musc*[1] provided by the OpenSim, and the simulation environment was developed in the MATLAB. The researchers used the model to simulate a PID control strategy that combines FES knee control with an active hip orthosis control in order to reproduce joint movements during gait. In this model, only the influence of the HNP was considered and the behavior of the patient was not take into account. This approach used by (SOUSA; FREIRE; BO, 2019) is the closest to the one used in this work.

Peña et al. (2019) used interaction model to estimate the torque performed by an user wearing an exoskeleton. The model was developed using the gait2392 musculoskeletal model from OpenSim and an EMG-driven Torque Estimation Environment was developed in MATLAB. According to the researchers, this approach is useful to implement an on-line adaptive control strategy for adjusting the robot assistance during the rehabilitation process.

Nunes, Santos e Siqueira (2018) developed a human-exoskeleton interaction control strategy based on kinetic motor primitives using interaction models. To this, the joint torques of an user with and without an exoskeleton were computed using the interaction model that was based on the gait2392 OpenSim model and scaled to a subject specific. Then, motor primitives were calculated using Principal Component Analysis (PCA). Finally the robot torques necessary to assist the patient were determined based on the weight of the motor primitives. The controller was applied to a knee exoskeleton and the experimental results showed that this method is efficient to recovery the movement profile of the patient.

[1] <https://simtk-confluence.stanford.edu/display/OpenSim/Musculoskeletal+Models>

Khamar e Edrisi (2018) designed an interaction control called backstepping sliding control (BSC) and a nonlinear disturbance observer (NDO) to apply on an assistant human knee exoskeleton. To test and validate the control and the observer, the researcher used an interaction model of the lower limbs, based on the Leg6Dof9Musc musculoskeletal model from OpenSim, and a simulation environment developed in the Simulink. Simulation results showed that the controller and observer are able to improve tracking accuracy and reduce the time required to eliminate disturbance.

Handford e Srinivasan (2018) used computational approach to simulate a interaction model of a transtibial amputee human walking wearing a robotic or passive prosthesis. In this model, an ideal actuator was modeled to provide torque to the prosthetic ankle joint. Four simple feedback controllers were used to control the active prosthesis. With this approach, the authors concluded that transtibial amputee walking gaits with left-right symmetry have higher metabolic rates than asymmetric gaits, suggesting a potential reason for asymmetries in amputee walking. The authors do not make clear which software they used to model and simulate the interaction model, which is a disadvantage of the work.

(NUNES et al., 2018) used interaction models to analyze the influence of an exoskeleton in the torques performed by an user wearing the robot. The interaction model was developed based on the gait2392 model from the OpenSim and the user torques were determined through the Inverse Dynamics Tool from the OpenSim. Experimental data from robot position and torque sensors were used to determine the patient's torque.

Guzmán et al. (2017) used computational simulation and interaction model to test and validate a control strategy for a hip–joint rehabilitation robot based on generalized proportional integral (GPI) controllers. The purpose of the controller was to guarantee the trajectory tracking task during a hip–joint rehabilitation in th presence of unknown disturbances. The simulations were performed in the MATLAB and MSC ADAMS simultaneously, the human being behavior was simulated as changes in the dynamics of the system. The results obtained through simulation using the interaction model was compared with the experimental ones and showed that the proposed GPI control has high performance and great potential for rehabilitation robotics.

An Adaptive Impedance Controller was developed by Peña (2017), where the robot's stiffness is varied according to the patient's stiffness. This controller was applied to an active knee orthosis, and the stiffness of the user was determined using an interaction model based on the neuromusculoskeletal computational model gait2392 from the OpenSim. In this case, the torque developed by the orthosis was applied to the interaction model and, through the Inverse Dynamics Tool from OpenSim, the user torque was determined serving to calculate the stiffness of the patient.

Ghannadi et al. (2017) developed a two-dimensional human-robot interaction model of the upper limbs. The model was accomplished through the MapleSim software and

simulated using the GPOPS-II optimal control package. A nonlinear model predictive control that has a feedforward and a feedback control loop was simulated: The feedforward commands are estimated using an internal representation of the arm, and the feedback control is a set of corrective commands resulting from sensory organs in the arm. This approach is close to the idea of human internal models and deals with the purpose of the present work..

Another work of Sousa et al. (2016) using interaction models was to compare performance of four types of controllers applied to Functional Electrical Stimulation Cycling (FES Cycling). In this work, the interaction model was developed using a lower limbs musculoskeletal model provided by OpenSim and the simulations were performed in the MATLAB. In this case, no type of orthosis was used and the interaction was test between the human being and the FES controllers.

Agarwal, Neptune e Deshpande (2016) developed a simulation framework using MATLAB and OpenSim, as a tool for designing, controlling, and testing of exoskeletons through simulation with coupled human–exoskeleton models. The framework allows the simultaneous modeling of the exoskeleton hardware and the musculoskeletal system, with the understanding of how the various system design and control parameters affect coupled system performance, in order to optimize exoskeleton designs to improve rehabilitation outcomes. Virtual experimentations were performed to different pathological conditions and the results demonstrated the features and applications of the proposed framework.

Handford e Srinivasan (2016) used interaction model in order to design a robotic ankle-foot prosthesis for amputees. The model consists of an amputee wearing an active ankle-foot prosthesis and simulations were made by simultaneously optimizing human movements and prosthesis actuation. Through the simulations, the authors tried to predict the user's walking kinematics as well as the metabolic cost involved, trying to minimize it by changing the dynamic characteristics of the prosthesis. Simulations using the interaction model (HANDFORD; SRINIVASAN, 2018) indicated that to minimize the metabolic cost the foot mass of the prosthesis should be decreased, however, the kinematics that demand less cost produces an asymmetrical gait.The use of computer models was a useful tool in prosthesis development, saving time and money. However, the authors do not make clear which software they used for modeling and simulation, which compromises the reproducibility of the project.

Durandau et al. (2016) used computational musculoskeletal model from OpenSim, scaled to specific subjects, in order to acquire muscle kinematics information to realize an EMG-driven model of human-machine interaction. This technique was experimentally applied to an individual wearing an exoskeleton in a real-time mode in order to estimates internal biomechanical variables from the user, allowing a better human-robot interaction.

Forward dynamics simulations were performed by LaPre, Umberger e Sup (2014)

using OpenSim in order to simulate an amputee human walking using a powered ankle prosthesis. The objective was to develop a prosthesis designed to dynamically align the tibia with the ground reaction force during the stance phase, avoiding damage of the soft tissue of the residual limb. To perform the simulations, the authors used the gait2354 neuromusculoskeletal model coupled to a computational model of the active prosthesis. Trough the simulation was possible to parametrize the orthosis, reducing the impact transferred to the remain tissue and improving the quality of life of the user.

Mansouri e Reinbolt (2012) developed an interface between OpenSim and MATLAB/Simulink in order to combine their relevant strengths, such as control systems development, rapid model-based design, numerical simulation and human movement dynamics reproduction. The program is based on the forward dynamics concept and was used by the researchers to simulate a closed loop PID controller of human arm model balancing a pole. The program was designed to receive control signals only for muscle actuators (i.e. muscle activations), so that human-robot interaction simulations with control signals for robotic actuators cannot be simulated.

Based on the aforementioned works, it is understood that several authors use modeling and simulation in the scope of robotic rehabilitation, but several works do not make clear which software was used to perform such modeling and simulations, which compromises the reproducibility of the projects. An analysis of the articles presented, the work of Sousa, Freire e Bo (2019) and Ghannadi et al. (2017) are the closest to this work in question: the first for the development of the model and the second for the simulation environment based on internal models.

3 METHODOLOGY

The development of this work can be divided into two principal stages: construction of the interaction model and elaboration of the simulation algorithm.

The interaction model consists of a computational model of the human neuro-musculoskeletal system, obtained from OpenSim, in which a computational model of an exoskeleton was coupled.

The simulation algorithm was developed at MATLAB and contains routines for robot control and emulation of human behavior. Such a program uses numerical integration to determine the movements performed by the human-robot model, based on force and torque inputs.

Both the model and the simulation algorithm were validated using data from experiments conducted at the Laboratory of Robotic Rehabilitation of the São Carlos School of Engineering, University of São Paulo. Finally, some interaction controls were simulated using the system.

In the following, the materials and methods used in the development of this work are presented in detail.

3.1 OpenSim

OpenSim [1] is an open-source and freely available environment for modeling, simulation and analyzing of the human movement developed in 2007 by Delp et al. (2007), which integrates models that describes the anatomy and physiology of the neuromusculoskeletal system with the multijoint-multibody mechanics.

The computational modeling and simulation provided by the OpenSim allows the researchers and clinicians to understand the mechanisms that are the base of movement disorders and design effective treatments in the area of rehabilitation medicine. Further, the software can be used to help development of robotic systems to assist the motion of humans, allowing researchers to understand how these devices interact with the neuromusculoskeletal system.

The OpenSim can provide modeling and simulation of the movement, but not the controllers (e.g. interaction control of a human-exoskeleton system), then, to fully satisfy the modeling-control-simulation triad, the software must be integrated with MATLAB, which allows to perform the necessary controls.

In this work, the OpenSim 3.3 is used to matches the anthropometry of neuromus-

[1] <http://opensim.stanford.edu>

culoskeletal models to a specific subject , calculate the torques necessary to perform a movement and simulate the controllers developed in MATLAB, providing data for analysis. The following is a description of the OpenSim resources used in this work.

3.1.1 Neuromusculoskeletal Models

To simulate the neuromusculoskeletal system (NMS) of the patients, two computer models of the human lower-limbs biomechanical system provided by OpenSim were used: *gait2392* [2] and *leg6dof9musc* [3].

The *gait2392* (Fig. 10a) is a three-dimensional, 23 degree-of-freedom model that has 92 musculotendon actuators to represent 76 muscles in the lower extremities and torso, the bones are modeled as rigid bodies. The default version of this model represents a subject with mass of 75.16 kg and a height of 1.8 m.

The *leg6dof9musc* (Fig. 10b) is a three-dimensional, 6 degree-of-freedom model with 9 musculotendon actuators and represents a single leg, pelvis, femur, tibia and foot.

In this work only three basic joints and their movements in the sagittal plane were considered: **hip, knee** and **ankle joints**. This consideration was made because the simulated exoskeleton deals only with movements in the sagittal plane of the joints in question.

Figure 10 – Neuromusculoskeletal models from OpenSim. The red lines are the musculotendon actuators.(a)Gait2392, (b)Leg6dof9musc.

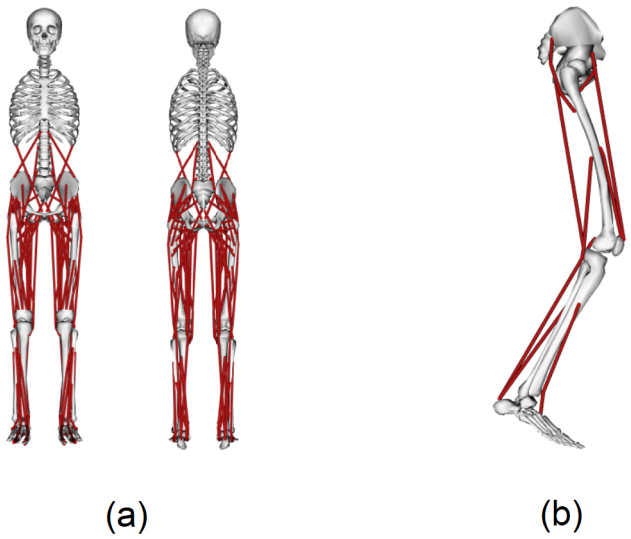

Source: Generated image from OpenSim 3.3.

[2] <https://simtk-confluence.stanford.edu/display/OpenSim/Gait%2B2392%2Band%2B2354%2BModels>

[3] <https://simtk-confluence.stanford.edu/display/OpenSim/Musculoskeletal+Models>

The OpenSim models were chosen because, besides representing well the biomechanics of human movements, it allows that external forces (e.g. torque from exoskeletons actuators) be coupled the models. This makes it possible to simulate patient interaction with the environment or other objects, such as a rehabilitation robot. In addition, the fact that the model has musculotendons actuators allows EMG or FES signals to be used in simulations, which is an advantage over models that have only mechanical representation of the human system.

Some features of the model can be edited through an xml editor (e.g. Notepad++ v7.5.6 [4]). In this work, this resource was used to add actuators to the joints of the model in order to represent the exoskeleton.

3.1.2 *Scaling*: Adjusting the anthropometrics characteristics of the model

To scale a neuromusculoskeletal model is to change its anthropometry so that it matches a particular subject as closely as possible. The *Scale Tool* of the OpenSim performs this model-subject combination by changing the dimensions and properties of body segments (mass, moment of inertia) as well as muscles and tendons.

Figure 11 – Virtual markers (red points) and experimental markers (blue points)

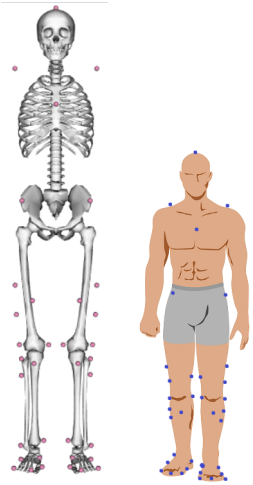

Source: Image generated by the author

Scaling is performed by comparing markers located at strategics points of the body (experimental marker data) with corresponding markers positioned on the model (virtual makers), Figure 11.

After obtained the scaled model, the inverse dynamics about a specific movement can be calculated, that is, the joint torques that the specific subject must perform to develop a given kinematics.

[4] <https://notepad-plus-plus.org/downloads/>

In this work, the scale tool was used to matches the NMS model with a subject specific that is able to use a real exoskeleton, in order to provide data capable of being validated experimentally.

3.1.3 *Inverse Dynamics*: Determining the generalized torques of the model

Inverse Dynamics deals with determining the forces and torques that a system must develop to perform a desired motion. This is achieved through resolution of the classical equations of motion that must be written in the following form:

$$M(q)\ddot{q} + V(q,\dot{q}) + F(\dot{q}) + G(q) + \tau_d = \tau \tag{3.1}$$

where $M(q)$ is the inertia matrix, $V(q,\dot{q})$ is the Coriolis/centripetal vector, $F(\dot{q})$ is the friction vector, $G(q)$ is the gravitational forces vector, τ_d are the external forces (e.g. Ground Reaction Forces, contact forces or another disturbances forces) and τ is the necessary forces/torque to develop the motion.

The *Inverse Dynamics Tool* of the OpenSim determines the generalized torques (i.e. the joint torques) necessary to develop a given movement, like to flex the knee or to take a step, by solving the equation above. The tool uses the kinematic of the movement (position, velocity and acceleration) and the external forces (e.g. ground reaction forces - GRF) to determine the net torques.

In this work, the Inverse Dynamics Tool was used to determine the torques developed by the user.

3.1.4 *Forward Dynamics*: Determining the motion of the model

In opposition to inverse dynamics where the motion of the model is known and we are interested in determine the forces and torques that generate the motion, the forward dynamics describes through a mathematical model of the dynamics of the mechanical system, how its coordinates and velocities changes when a force or torque is applied to its joints.

Solving the equation below, the acceleration $\ddot{q}$ of the joints are determined. Then, through numerical integration, velocities and positions can be found for each instant of time during movement execution.

$$\ddot{q} = [M(q)]^{-1}(\tau - V(q,\dot{q}) - F(\dot{q}) - G(q) - \tau_d) \tag{3.2}$$

The *Forward Dynamics Tool* of OpenSim determines the generalized acceleration, velocities and positions of the NMS when torque or muscles excitations are applied in its joints or musculotendons, respectively.

In this work, the Forward Dynamics Tool from the OpenSim was not used: a forward dynamics-based routine was developed in MATLAB. This was made because the tool of the OpenSim is not able to reproduce feedback controls during its execution, and since many interaction controls as well as human control have a feedback loop, the MATLAB routine had to be developed.

3.2 Exoskeleton - ExoTao

The virtual exoskeleton developed in this work and coupled to the NMS was based on the exoskeleton for lower limbs, ExoTao, introduced by Santos et al. (2017) (Fig. 12). The ExoTao is constituted of a lightweight tubular structure, with six independent and free joints which provide a modular feature to the robot. These features allow the exoskeleton to be configured to treat one or more joints of the patient.

The actuation of the robot can be performed actively through use of actuators (i.e. motor coupled to a gearbox), or passively, by means of springs and dampers.

In addition, the telescopic tubular links of the robot allows to adjust its size in order to fit it to a specific subject, aligning the joints of the exoskeleton with the patient ones. The system is adjustable for patients with body height between 1.65 and 1.90 m.

In this work the ExoTao was used to perform some experiments in order to generate data em validate the model proposed.

Figure 12 – User wearing the complete ExoTao.

Source: (SANTOS et al., 2017)

3.2.1 Virtual Exoskeleton

A computational model of an exoskeleton was coupled to the NMS model in order to provide the human model with the external joint torques generated by a real exoskeleton of lower-limbs.

The exoskeleton model was created by editing the NMS model and including in the joints of the hip, knee and ankle *coordinate actuators* capable of performing an angular movement in the sagittal plane and representatives of the actuators (motor + reduction set) of the real exoskeleton (Fig. 13).

A coordinate actuator is a virtual actuator of the OpenSim that applies a generalized force (or torque) to a generalized coordinate. The force applied by the actuator is proportional to its input control signal, as expressed in equation (3.3).

$$\tau = u \cdot \tau_{optm} \tag{3.3}$$

where τ_{optm} is the maximum torque (optimal torque) that the actuator can apply (specific for each joint and control) and u is the control signal that varies between -1 and 1.

In this work, this type of actuator was chosen because of its functional similarity with the exoskeleton actuators: generalized torque application for sagittal plane movements.

Figure 13 – NME with exoskeleton. The yellow arrows indicate the locations of the coordinate actuators.

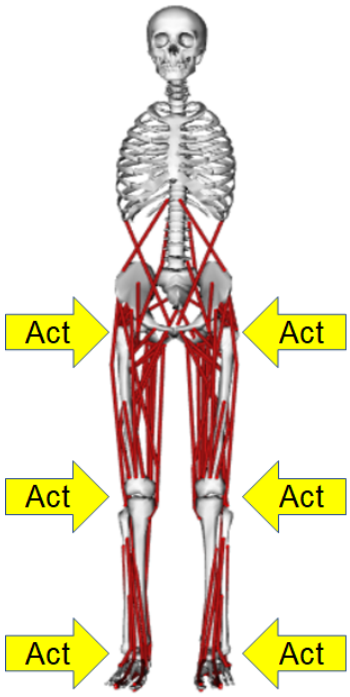

Source: Image generated by the author

At first, there is no pictorial representation of the actuators, so that only their functional characteristics will be coupled to the NMS model. During the scaling, the total mass of the interaction model was increased in 8 kg, in order to represent the mass of the exoskeleton ExoTao with it actuator.

Some simplifications are considered: the actuators have no delay in response and no losses, the axes of the joints of the robot and the user are collinear and the torque is applied directly to the human joint in question. The ankle was locked at a 90 degree angle. In order to reduce complexity and computational cost, the muscles were not used as actuators in this experiment, so that all the torque involved (both user and robot) was delivered to the model through the coordinate actuators.

3.3 Forward Dynamics Based Simulation Environment

In order to reproduce the interaction controls, an algorithm based in forward dynamics was developed, combining the capabilities of modeling and simulation of the OpenSim with those of control of the MATLAB.

The program was developed in MATLAB using the OpenSim API in order to access the OpenSim and Simtk libraries where are the models and some specifics particular functions (e.g. functions to access the states of the model). The source code was based on the one developed by Dembia (2014). A flowchart of the program can be observed in the Fig. 14.

Figure 14 – Forward Dynamics Based algorithm to simulation the interaction controls applied to the human-exoskeleton interaction model.

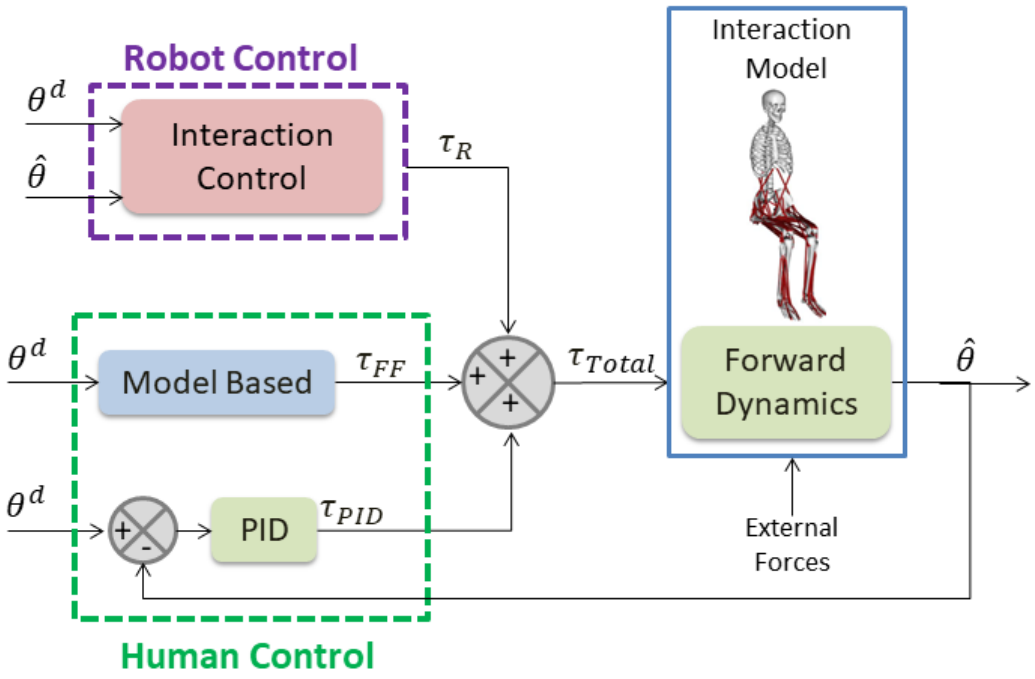

Source: Image generated by the author

The **Robot Control** is the loop that contains the interaction control (e.g. impedance control, fuzzy control, primitive-based control) that governs the actions of the exoskeleton. Its inputs are the desired position of the joints (θ^d) and the real position of the joints ($\hat{\theta}$). The output are the torques of the robot actuators (τ_R).

The **Human Control** simulates the human behavior, and is based on the feedforward-feedback control and internal model concept with a feedforward loop that estimates the torque required (τ_{FF}) to perform a desired movement (θ^d), and a feedback loop that apply a correction torque (τ_{PID}) in order to eliminate the tracking errors. In this work, the feedforward loop consists of the Inverse Dynamics Tool from OpenSim and the feedback loop is a conventional proportional-integral-derivative control whose the law is expressed by the Eq. (3.4).

$$u = K_p e(t) + K_i \int_0^t e(\tau)d\tau + K_d \frac{de(t)}{dt} \tag{3.4}$$

where $e(t)$ is the position error: $e(t) = \theta_r(t) - \hat{\theta}(t)$ and K_p, K_i and K_d are the proportional, integral and derivative gains respectively.

Unlike the concept of the internal model presented in Section 2.2, in this work the internal model (represented by the Inverse Dynamics Tool from OpenSim) is static and does not evolve over time.

The torques from robot and the ones from the user are summed resulting in a **torque total** (τ_{Total}) that is applied in the coordinate actuators of the interaction model. Then, the Forward Dynamics routine (green rectangle in the Fig. 14) determines the real position of the joints ($\hat{\theta}$), realizing the integration of the dynamics equations of the model, considering the inputs of torque total and the external forces. The integration routine use de ODE45 from MATLAB.

The **External Forces**, as its name says, are forces that do not come from the human-robot system, but come from another sources like as the ground (ground reaction forces), additional loads placed by the therapist, and contact forces with the environment.

It is important to note that the Interaction Control, the Model Based feedforward loop and the feedback PID loop can be can be replaced by models different from those used in this work, according to the needs and interest of the rehabilitation engineer and therapist.

In this work, all the simulation were performed on a computer with Intel®Core™i7-5500 2.40 GHz processor, 8,00 GB of RAM, 2,00 GB dedicated video card, Windows 10 Home Single Language 64 bits. The OpenSim version 3.3 and the MATLAB R2017b were the platforms where the simulations took place.

3.4 Validation of the System

In order to study and validate the interaction model and the simulation environment, data from an experiment developed by (PEÑA et al., 2019) were used. The experiment consists of an user wearing the active knee orthosis in a seated position performing active movements (Fig. 15).

The desired trajectory that the user attempted to execute correspond to a sinusoidal signal with an amplitude of $-90°$ (knee flexed) to $0°$ (knee extended). A low level impedance control was used in the robot and the experiment was divided in two phases, according to the variation of the stiffness K_{exo} of the impedance control of the orthosis:

- Phase 1: User is active, robot is active with stiffness $K_{exo} = 60$ Nm/rad;
- Phase 2: User is active, robot is active with stiffness $K_{exo} = 60$ Nm/rad, with a $180°$ phase shift in the desired trajectory of the robot.

In Phase 1 the orthosis assumes an assistive behavior and in Phase 2 it presents itself resistive to the movement performed by the user.

Figure 15 – Flowchart of the validation procedure algorithm.

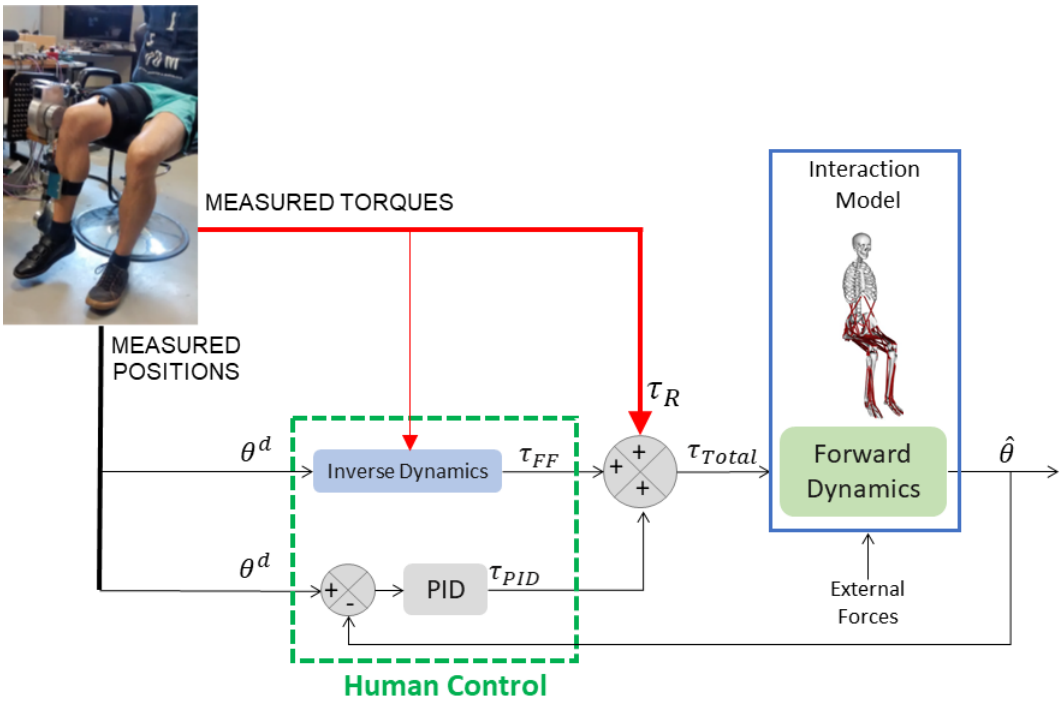

Source: Image generated by the author

The torque developed by the robot (τ_R) and the knee position (θ^d) were measured during the experiment. After, this data were utilized to determine the torque developed by the user (τ_{FF}), using the Inverse Dynamics Tool.

Having the measured torque and position from the experiment, and the estimated user torque from the Inverse Dynamics, the simulation was performed using the knee position measured as the trajectory reference: the objective was to verify if the model, with the torques measured and estimated, was capable of performing the same movement measured during the experiment, that is, $\hat{\theta} = \theta^d$ being the $\hat{\theta}$ the variable determined computationally through the simulation, and θ^d the measured position from the experiment performed with the user wearing the exoskeleton.

3.5 Human-robot Interaction Controls Tested

After validating the model and the simulation environment, four interaction controls were simulated, namely:

Impedance Control: In this simulation, the interaction model was based on the NMS *gait2392* and performed movements only with the right knee, in a seated position. A robotic actuator in the knee (representing the active knee joint of the ExoTao) governed by a impedance control law, provided the interaction torque in three ways: passive,

active-assistive and active-resistive. The results are presented in the Section 4.2.

Fuzzy-based Adaptive Impedance Control: In this case, the interaction model and the motion were the same of the simulation described above. But in this case the stiffness in the control law was changed by a fuzzy inference, based on the position error and user torque. This variation in gain implies a variation in the assistance provided by the robot to the user during therapy. The results are presented in the Section 4.3.

Motor Primitives-base Control: This control based on the motor primitives seeks to make the exoskeleton transparent to the user, that is, the user must not apply any additional force or torque when using the robot. The interaction model and the movement were the same of the previous simulations. The results are presented in the Section 4.4.

Simulating the Gait Swing Phase: In this case, the interaction model used was based on the *leg6dof9musc* and the motion performed represents the leg during the swing phase of a step. This test was divided in three stage: the first to adapt the model and adjust the PID gains, the second to validate the system and the third to simulate an impedance control. The results are presented in the Section 4.5.

More details about these tests are presented in the Section 4, with the results obtained with the simulation. This way, you will avoid having to go back to this section when you read the results section.

4 RESULTS

This chapter will present the results from the model validation and from the simulations of various interaction controls. For the 4.1 section, keep in mind Figure 15, for the other sections, see Figure 14. These figures contain the flowcharts of the simulation programs pertinent to each case.

In an unconventional way, the details of the simulations and procedures performed are presented in this section, rather than in the methodology.

The intention of using this approach is to make reading easy both for those who are reading the text completely and directly, and for those who interested only in a specific point, thus avoiding the reader having to move between chapters.

4.1 Validating the Interaction Model and the Simulation Environment

The procedure to validate the interaction model and the simulation environment was presented in the section 3.4: using data from a physical experiment, a simulation was performed to make the model reproduce the same movements performed by the user during the experiment.

Remember: the tests were performed in two phases: **Phase 1** where the robot behavior during the physical experiment is active-assistive and **Phase 2** where the robot behavior is active-resistive. The joint position of the exoskeleton measured experimentally was used as reference input (θ^d) to the simulation algorithm, and was expected to be equal the movement performed by the interaction model ($\hat{\theta}$).

The angular position measured from the robot was well tracked by the interaction model during the computational simulation (Fig. 16 and Fig. 18). An analysis of the tracking error is presented in the Table 1. Considering all the uncertainties of modeling, computational integration and experimental data collection, the error obtained is tolerable and the $\hat{\theta}$ is satisfactory.

Table 1 – Knee angular position error analysis.

Error [deg]	Phase 1	Phase 2
RMS	0.783	0.755
Maximum positive	1.235	2.281
Maximum negative	-1.694	-1.985

$error = \theta^d - \hat{\theta}$

Figure 16 – Analyze of the angular position of the phase 1. (Knee Real = $\hat{\theta}$ and Knee Reference θ^d).

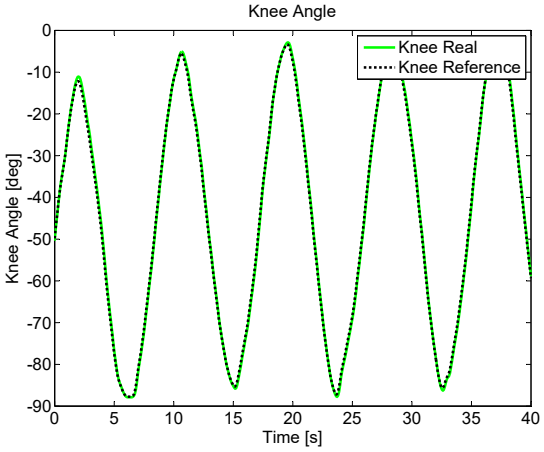

Source: Image generated by the author

Figure 17 – Analyze of the tracking error of the phase 1. ($\theta^d - \hat{\theta}$). RMS error = 0.783°.

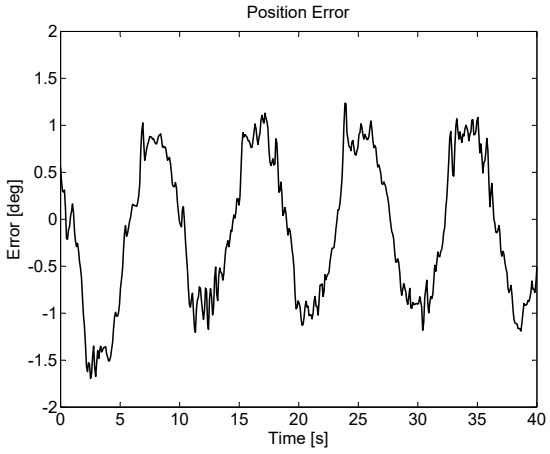

Source: Image generated by the author

Figure 18 – Analyze of the angular position of the phase 2. (Knee Real = $\hat{\theta}$ and Knee Reference θ^d).

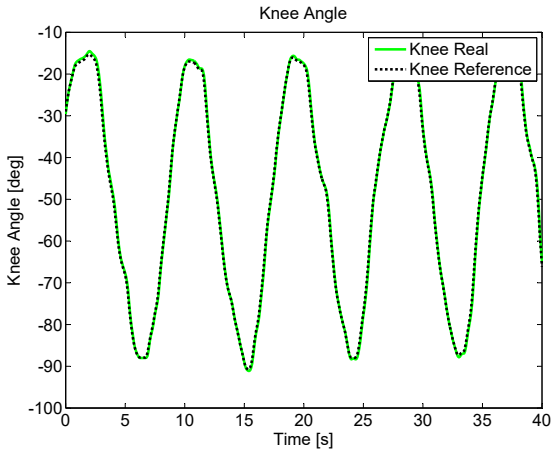

Source: Image generated by the author

Figure 19 – Analyze of the tracking error of the phase 2. ($\theta^d - \hat{\theta}$). RMS error = 0.755°.

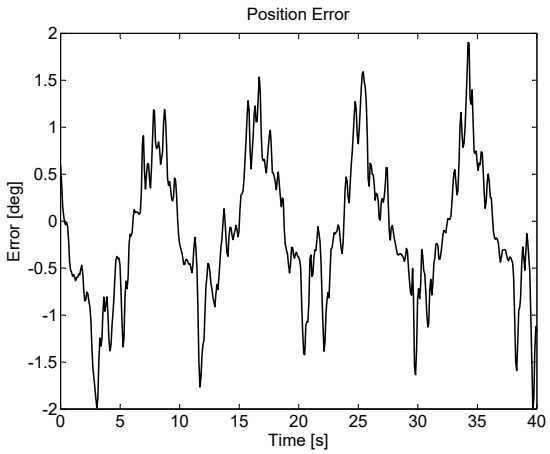

Source: Image generated by the author

The figures 20 and 21 shown the torques involved in the phases 1 and 2, respectively. The red line ares the torque applied by the exoskeleton through the interaction control, the black line is the torque estimated by the user through the internal model from feedforward loop (in this case, modeled through the Inverse Dynamics Tool), the green line is the torque developed by the user through the feedback PID loop, in order to eliminate the disturbances that prevent the good tracking of the desired trajectory, and finally, the blue line is the sum of all the torques involved in the motion: both the robot and the user.

Remember: the robot torques were measured during the physical experiment of an user wearing the exoskeleton, and the user torques were determined computationally, during the simulation.

As can be seen, the torque from the PID loop is noisy even though it is wrapped around the zero line. This is mainly due to the noise present in the data collection, which, despite all the filtering involved, could not be completely eliminated. Other uncertainties related to the anthropomorphic adaptation of the model to the user and the computational numerical integrations contributed to a noisy profile in the PID torque.

In phase 1 the torque applied by the robot is assistive and has a small amplitude when compared to the torque developed by the user (Fig. 20). In phase 2, the torque applied by the robot is resistive having a 180 degrees shift in relation to the user torque, what can be seen in the Fig. 21.

Figure 20 – Torques of the Phase 1.

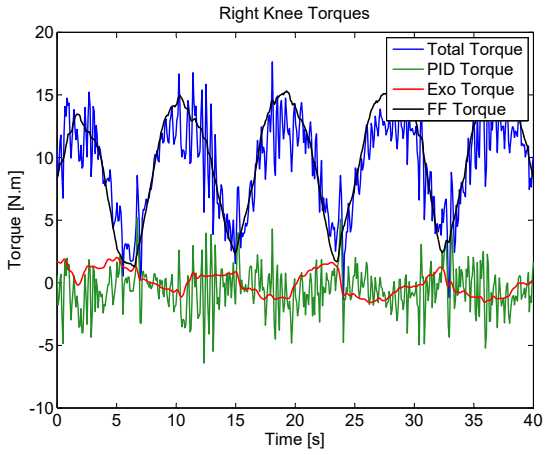

Source: Image generated by the author

Figure 21 – Torques of the Phase 2.

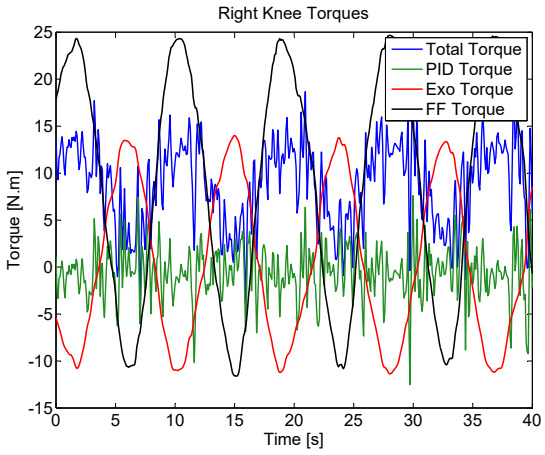

Source: Image generated by the author

Despite the noisy profile of the PID torque, the interaction model reproduced well the movement performed by the user during the physical experiment, and the simulation environment worked well showing that the forward dynamics approach is effective. Thus, both the model and the proposed simulation program were considered validated and then tested with other interaction controls, as will be presented in the next topics.

Each simulation took 14 minutes to complete, so that in half an hour the model and the simulation environment were validated.

These results were published in the 25^{th} ABCM International Congress of Mechanical Engineering (MOSCONI et al., 2019).

4.2 Impedance Control

An impedance-based interaction control with the control law expressed by the equation (4.1) was simulated. The torque developed by the robot is based on the position error and the angular velocity of the joint.

$$\tau_R = K_{exo}\theta_e - B_{exo}\dot{\theta} \tag{4.1}$$

where τ_R is the torque developed by the exoskeleton, $\theta_e = \theta^d - \theta$ is the position error, $\dot{\theta}$ is the angular velocity of the joint and K_{exo} and B_{exo} are stiffness and damping parameters.

Four tests were performed, varying in each of them the impedance and behavior of the robot (passive, active-assistive, active-resistive). For all tests the B_{exo} value was kept constant and equal to 0.01 N.s/rad. Only the right knee joint was used in the tests and the model remained in a seated position (i.e. no ground reaction forces present) performing active movements according to a sinusoidal desired trajectory with an amplitude of $-70°$ (knee flexed) to $-20°$ (knee extended). The interaction model was based on the NMS *gait2392*.

Figure 22 – Movement performed during the tests.

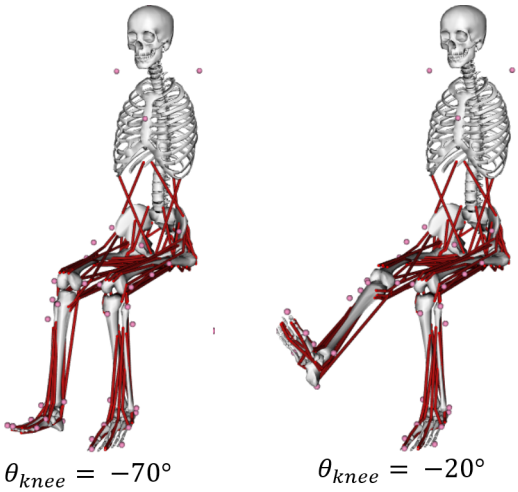

Source: Image generated by the author

As mentioned above, there are no ground reaction forces, however, a constant torque of 6 N.m was applied to the patient's knee, without his knowing beforehand, representing a disturbance such as a static charge inadvertently applied by the therapist, so that the user reacts to this unexpected disturbance by applying a compensating torque through the feedback control.

Test 1: $K_{exo} = 0$, robot is passive. In this case the patient developed all the torque necessary to perform the movement and correct the error caused by disturbance.

Test 2: $K_{exo} = 62.5$, robot is active-assistive. The robot assists the patient in performing the movement.

Test 3: $K_{exo} = 62.5$, robot is active-assistive. This is a repetition of the previous test, but in this case the patient was adjusted to present a weakness in the knee, requiring further assistance from the robot. The weakness was modeled as a boundary in the maximum total torque that the user can to perform.

Test 4: $K_{exo} = 6.25$, robot is active-resistive. The desired trajectory of the robot has a 180 degrees phase shift, so that the exoskeleton behaves resistively, opposing the patient's movement, requiring the user to employ even greater torque to perform the task.

In Test 1 there was a position error at the beginning of the movement which was corrected over time due to the user feedback control action, which converged to 6 N.m, equivalent to the applied static load (figures 23 and 24).

Figure 23 – Position of the Test 1.

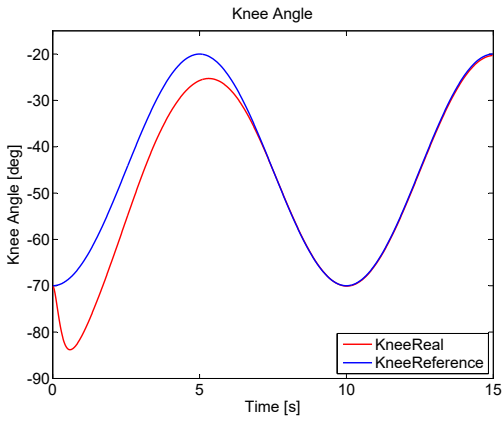

Source: Image generated by the author

Figure 24 – Torques of the Test 1.

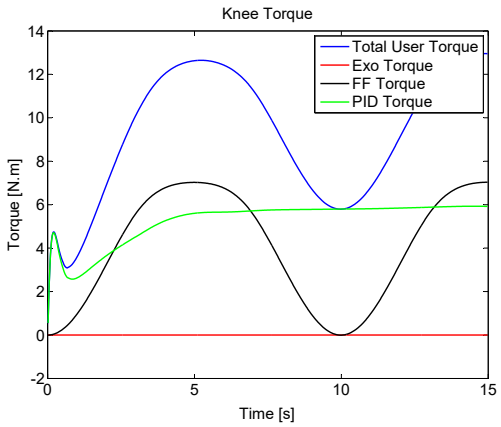

Source: Image generated by the author

In Test 2, the robot assists the patient in performing the movement when the position error is large. As the error is extinguished over time, the robot reduces the amount of assistive torque delivered, remaining only the user-developed torque, which proves that the control is capable of meeting the assist-as-needed paradigm (figures 25 and 26).

Figure 25 – Position of the Test 2.

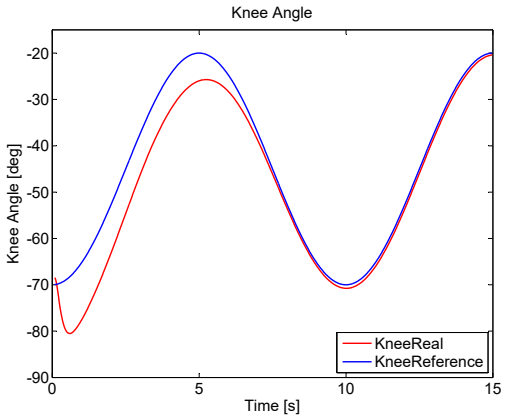

Source: Image generated by the author

Figure 26 – Torques of the Test 2.

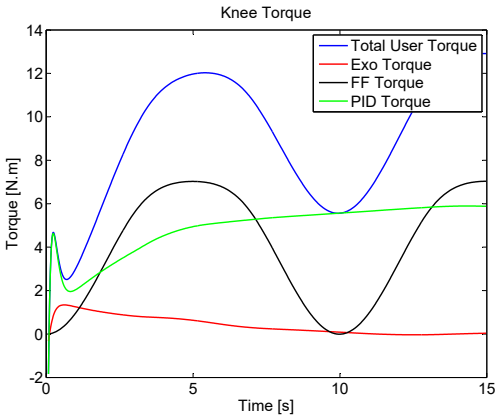

Source: Image generated by the author

Test 3 reaffirms what was observed in Test 2. In this case the robot maintained the assistive torque, since the patient could not perform the movement because of the simulated muscle weakness. The initial conditions of the simulation caused initial oscillations which can be disregarded in this case (figures 27 and 28).

Figure 27 – Position of the Test 3.

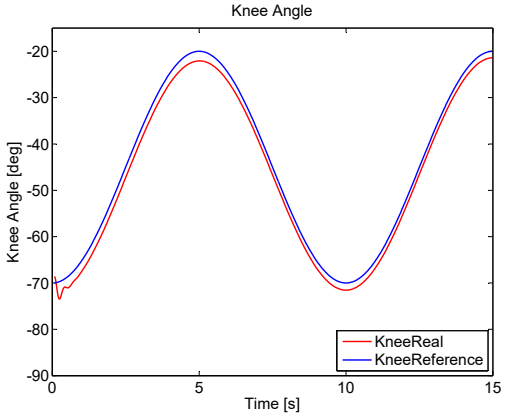

Source: Image generated by the author

Figure 28 – Torques of the Test 3.

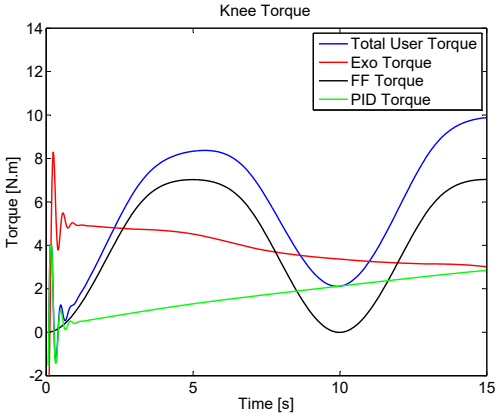

Source: Image generated by the author

In Test 4, the robot assumes a resistive behavior, which can be observed by comparing the robot's torque to the user's total torque. Position errors are caused which the patient attempts to eliminate by applying a feedback control torque. Here the correction torques are based on the calculated position error, but in practice these torques are produced by the user based on the afferent signals that indicate how the movement is being performed in relation to the desired one. based on afferent signals (e.g. vision, touch). In this case,

the same control law was used, varying only the robot's reference trajectory in relation to the user's one.

Figure 29 – Position of the Test 4.

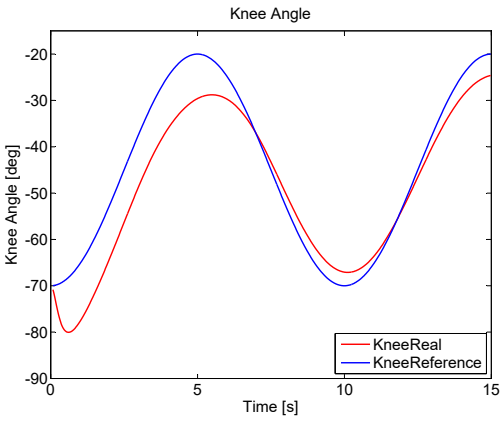

Source: Image generated by the author

Figure 30 – Torques of the Test 4.

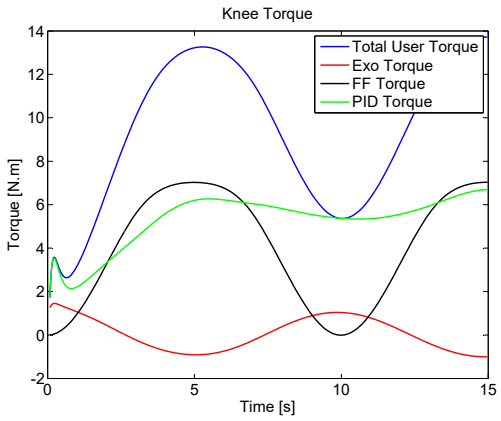

Source: Image generated by the author

Each simulation took about 5 minutes to prepare and 25 minutes to complete, so all four tests were prepared and performed for a total of 2 hours. Physical experiments performed with the same protocol would take much longer.

These results were published in the XIV Conferência Brasileira de Dinâmica, Controle e Aplicações (MOSCONI; SIQUEIRA, 2019).

4.3 Fuzzy-based Adaptive Impedance Control

An adaptive control that makes the robot automatically vary the amount of assistance to the user during therapy was simulated. The control law of the interaction control is given by

$$\tau_R = K_{exo}(\theta^d - \hat{\theta}) - B_{exo}\dot{\theta} \tag{4.2}$$

where B_{exo} the damp coefficient of the exoskeleton, constant and equal to 0.01 N.s/rad and K_{exo} is the robot stiffness that is variable according to a fuzzy logic inference. The variation of K_{exo} is directly proportional to the level of assistance that the robot provides to the user and seeks to meet the *assist-as-needed* paradigm.

For this purpose, the inputs for fuzzy inference are the RMS **position error** and **user torque**, normalized to predetermined maximum values according to the Equation (4.3) and the output is the stiffness K_{exo}.

$$\tilde{x} = \frac{1}{x_{max}} \sqrt{\frac{1}{N} \sum_{i=1}^{N} x_i^2} \tag{4.3}$$

where the variable x is the variable of interest (position error or user torque), N is the number of samples to calculate the root mean square, x_{max} is the maximum value to the normalization and $\tilde{x}$ is the variable normalized.

For fuzzification and defuzzification five symmetric triangular membership functions were defined to each input/output, classifying them as Very Low (VL), Low (L), Medium (M), High (H) and Very High (VH).

Figure 31 – Input membership for fuzzification.

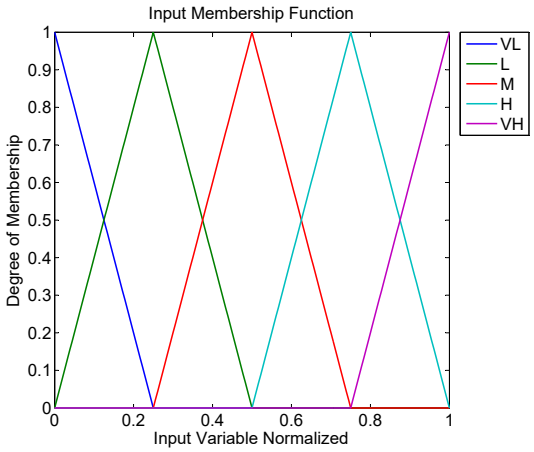

Source: Image generated by the author

Figure 32 – Output membership for defuzzification.

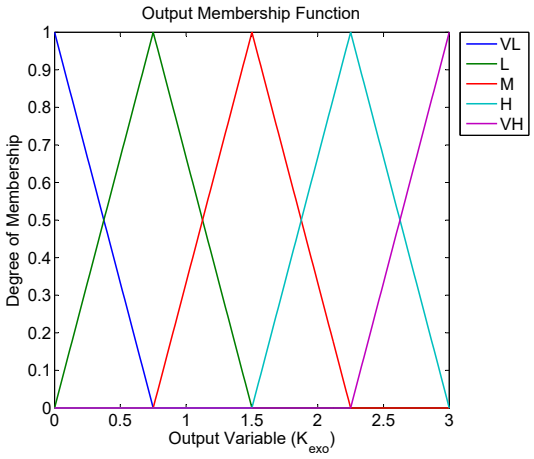

Source: Image generated by the author

The fuzzy rules for impedance adaptation were formulated in order to meet the assist-as-needed paradigm and are presented in the Table 2. The output inference is determined through the Mamdani fuzzy implication and the Max-Min method. The defuzzification is performed through the center-of-area method and the output surface can be seen in Figure 33.

Two tests were performed considering the model in a sitting position, using only the knee joint of the exoskeleton and performing a movement of flexion and extension of the right knee, following a sinusoidal trajectory. In this condition the model does not suffer action of the ground reaction forces and the external forces were considered null. The interaction model was based on the NMS *gait2392*.

Table 2 – Impedance adaptation rules, the Authors (2019).

		τ_{user}				
		VL	**L**	**M**	**H**	**VH**
$\dot{\theta}$	**VL**	L	L	L	VL	VL
	L	M	M	L	L	VL
	M	H	M	M	L	L

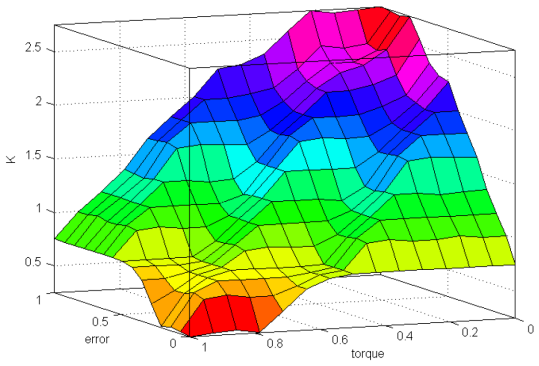

Figure 33 – Surface of the fuzzy-based adaptive impedance. The Authors (2019).

In the first test (here referred to as Test 1), was considered only the user, without the exoskeleton, then, all the torque employed to perform the motion was developed by the subject. In the second test (here referred to as Test 2) the robot was utilized with the adaptive impedance control presented above, in this case the torque involved in the realization of the movement was provided by both the user and the robot.

In both tests, the user was simulated as a patient with some muscular weakness and unable to develop the necessary torque to perform the movement without tracking errors in relation to the desired positions.

Figure 34 – Knee position of Test 1 (without exo).

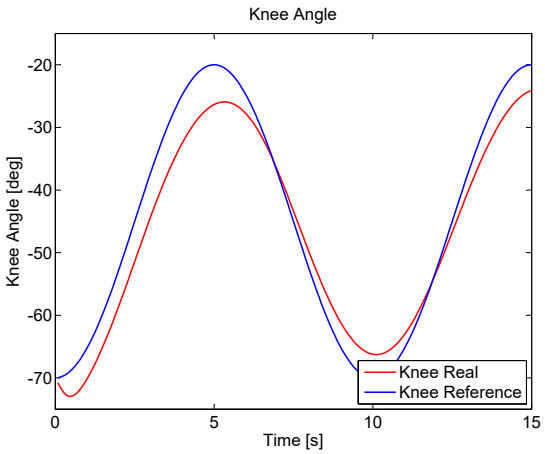

Source: Image generated by the author

Figure 35 – Knee position of Test 2 (with exo).

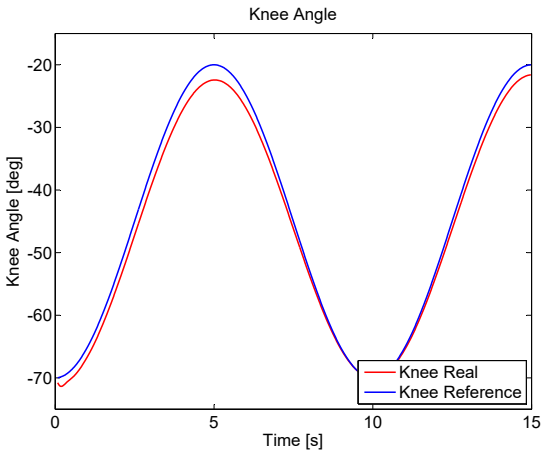

Source: Image generated by the author

Analyzing the graphs in figures 34 and 35, it is possible to verify that the patient can follow the movement shape determined by the reference trajectory, but cannot perform

the movement accurately when doing it alone. Using the robot ensured that the patient could complete the movement with minimal error.

Figure 36 – Comparison between the position errors of the both tests.

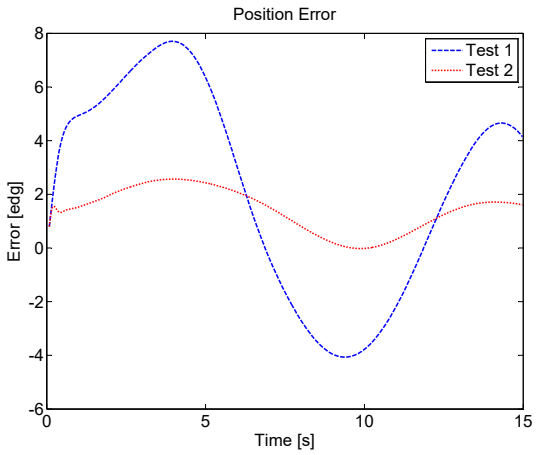

Source: Image generated by the author

The tracking errors were reduced with the assistance of the robot, as can seen in the Figure 36. The RMS position errors were 4.46° for the first test, and 1.64° for the second one.

Figure 37 – Knee torques of Test 1 (without exo).

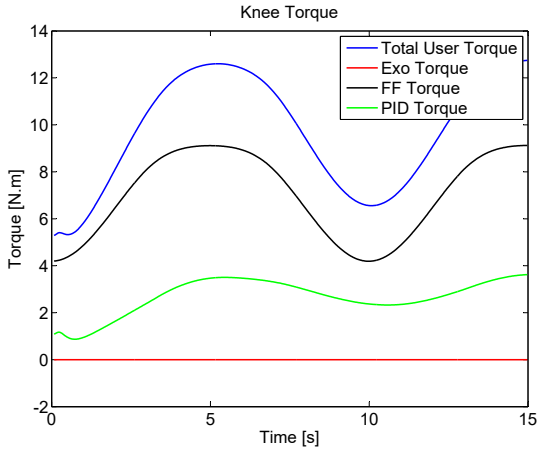

Source: Image generated by the author

Figure 38 – Knee torques of Test 2 (with exo).

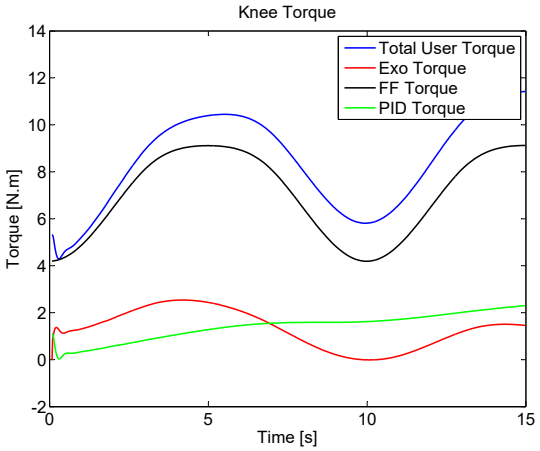

Source: Image generated by the author

Although the patient performs a larger modulus effort when not wearing the robot (Fig. 37), such effort is not well oriented so that there are tracking errors, as can be seen in

Figure 34. The robot assists the patient in guiding the application of force, assisting him to perform the movement correctly and preventing muscle fatigue due to overexertion.

Importantly, treatment seeks to reestablish the patient's movement pattern and motor coordination, so that performing standardized movements is more important than performing high effort.

According to the graph in Figure 38, it is possible to verify that the robot provides a torque whose sinusoidal shape matches the desired movement.

Figure 39 – Virtual stiffness of the robot, modulated according to the fuzzy inference.

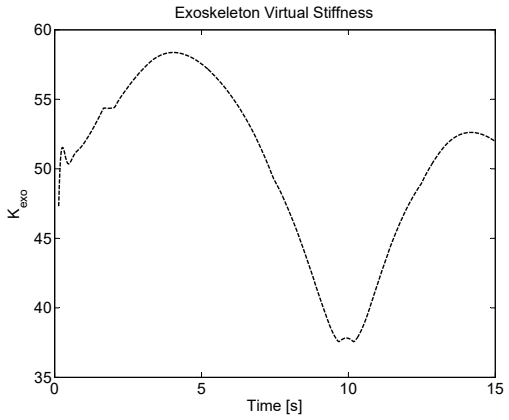

Source: Image generated by the author

The stiffness of the robot (Fig. 39) depicts the level of user assistance, which decreases along the movement as the error approaches zero. This fact can be proved by checking the torque provided by the robot, which also approaches zero, so that the exoskeleton acts only by assisting the patient to perform the desired motion shape well, without making the movement by the user.

The two tests took 19 minutes each to be computationally simulated, so that in less than one hour the proposed control can be verified and compared with a similar situation, but without robot assistance. Other tests can be performed, such as keeping the stiffness constant or making the robot act in active-resistive mode, these changes only take a few minutes to set up and less than half an hour to test, which is not possible with laboratory tests using the actual exoskeleton and user.

These results were published in the IV Simpósio do Programa de Pós-Graduação em Engenharia Mecânica (MOSCONI; NUNES; SIQUEIRA, 2019).

4.4 Motor Primitives-based Control

A transparency control based on the motor primitives, developed by (NUNES; SANTOS; SIQUEIRA, 2018), was simulated. The purpose of this control is to ensure the

user performs the same effort wearing or not the exoskeleton, that is, the robot should only perform a torque that compensates for its own inertia and mass.

In this case, the user was considered a healthy subject, remaining in a seat position and performing sinusoidal movements of extension and flexion of the right knee joint. In this simulation, the control was performed focusing only on transparency, not rehabilitation. The interaction model was based on the NMS *gait2392*. The interaction control law is given by:

$$\tau_{exo} = \sum_{i=1}^{n} p_i^{wo}(1 - \vartheta)w_i^{wo} \tag{4.4}$$

$$\vartheta = \frac{w_i^w}{w_i^{wo}} \tag{4.5}$$

where τ_{exo} is the torque that the robot should to perform, compensating its inertia and mass, ensuring the transparency. p_i^{wo} and w_i^{wo} are the primitives and the torques weights of the subject without the orthosis. w_i^w are the torque weights of the user wearing the exoskeleton. For more information on the development of this control, see (NUNES; SANTOS; SIQUEIRA, 2018). Using the *Scale Tool* from OpenSim, the interaction model was scaled to a subject of 1.80 m height and with a mass of 80 kg.

As can be seen in Figure 40, the model correctly followed the reference trajectory. Analyzing Figure 41, it can be seen that the user performs the same torque wearing or not the exoskeleton (coincident green and black lines), that is, at all times it seems to the user that he is without the orthosis (this is the concept of transparency control). To make this possible, the robot has developed a compensation torque (red line). If the robot did not produce this compensatory torque, the user should perform the total torque (blue line) to transport his own weight plus that of the robot.

Figure 40 – Knee position with the motor primitive-based control.

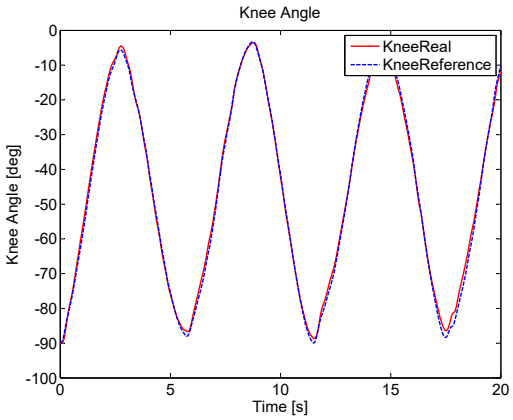

Source: Image generated by the author

Figure 41 – Torques analysis with the motor primitive-based control.

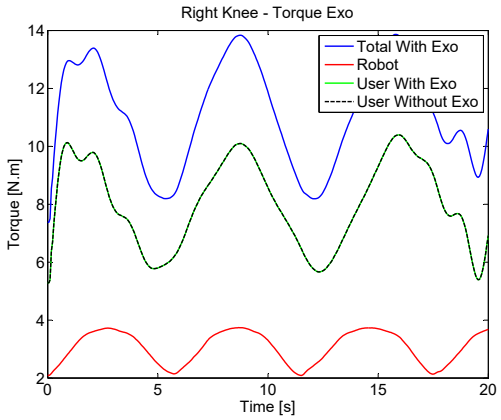

Source: Image generated by the author

In Figure 41, With regard to the user's torque, only the total torque component was shown (green and black lines), and the feedforward torque and feedback were not discriminated, in order not to compromise the readability of the data.

These results were published in the X Congreso Iberoamericano de Tecnologias de Apoyo a la Discapacidad (NUNES; MOSCONI; SIQUEIRA, 2019).

4.5 Simulating the Gait Swing Phase

Three simulation were performed using the interaction model based on the NMS *leg6dof9musc*. The purpose of the first simulation was to adapt the model and adjust the PID gains, the second simulation was performed to validate the model and the third one was performed to reproduce an impedance control.

To adjust and validate the interaction model and the simulation algorithm, a person wearing the ExoTao walked on a treadmill at a speed of 2 km/h for 3 minutes, with the torque and position of the robot joints being measured. An impedance control expressed by (4.6) determined the torque of the ExoTao during the physical experiment:

$$\tau_R = K_{exo}\theta_e - B_{exo}\dot{\theta} \tag{4.6}$$

As no measurement of ground reaction forces was performed during the experiment, only the swing phase was analyzed, when there is no interference from these forces. For that, the position and torque values of the execution of ten steps were used to determine an average value of these variables (Fig. 42). Then, the graphic resources of OpenSim were used to determine the swing and stance phases. Finally, the balance phase was extracted from the total step cycle and used in the validation and test simulations.

Figure 42 – Average position of the hip and ankle joints during the execution of 1.5 steps.

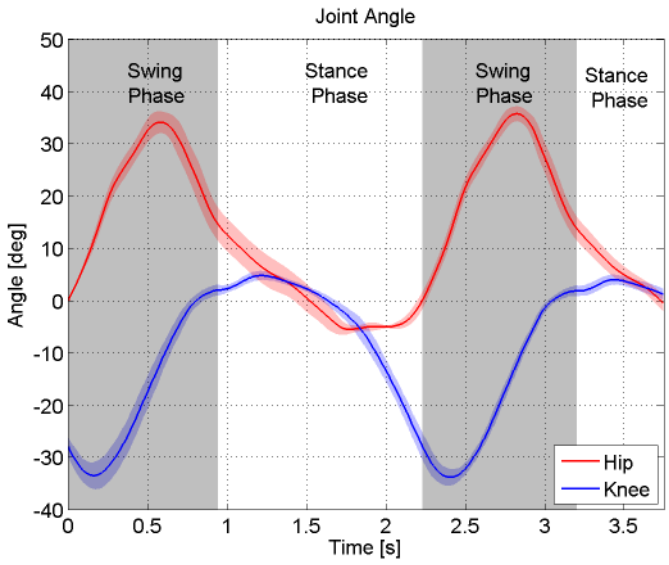

Source: Image generated by the author

In all the simulation, the ankle joint was locked at a 90 degree angle, simulating the effect of a passive orthosis.

Next, each of the simulations will be presented in detail, together with the results obtained in each one.

4.5.1 Stage 1: Adjusting the model and the PID

In this moment, the measured robot torque (τ_R) was used to determine the forward user torque (τ_{FF}) through the Inverse Dynamics Tool from OpenSim, and as an input to the forward dynamics-based algorithm (Fig.43). The measured robot position (θ_R) was used as the reference input to the simulation algorithm (θ^d).

It was expected that, with the simulation, the interaction model would perform the same movement that the subject performed during the physical experiment, that is, $\hat{\theta} = \theta^d$ (which means $\hat{\theta} = \theta_R$).

In this case, the stiffness of the impedance control of the ExoTao (Eq. (4.6)) was $K_{exo} = 30$.

Figure 43 – Forward Dynamics Based algorithm to simulate the interaction controls applied to the human-exoskeleton interaction model.

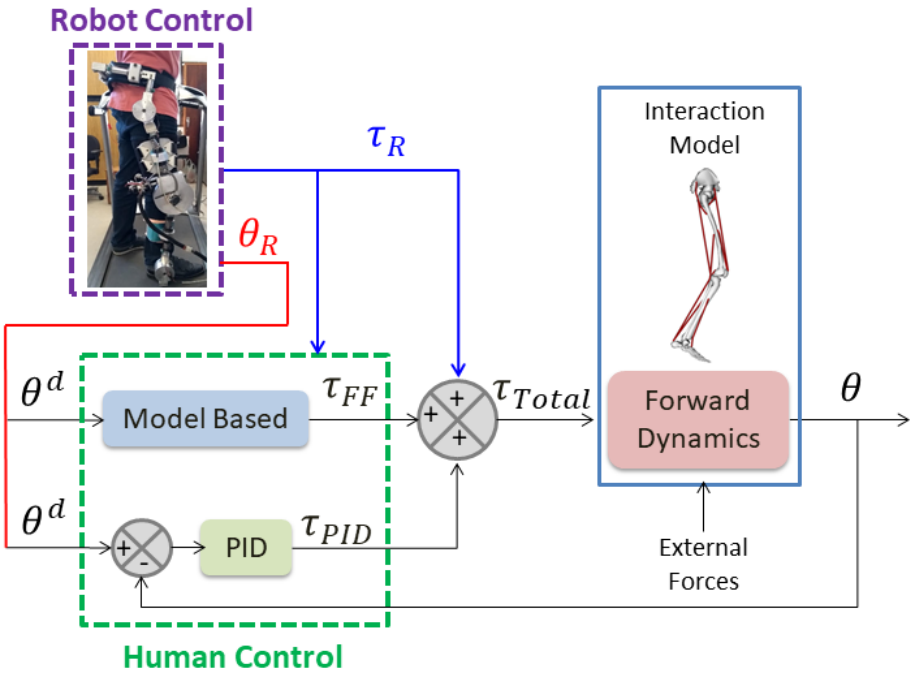

Source: Image generated by the author

After adjusted both the model and the gains, the results obtained were satisfactory, with the interaction model tracking the reference as can be seen in the Figures 44 and 45. As expected, the interaction model managed to perform the same movement as the user walking on the treadmill.

Figure 44 – Joint position after adjusts. (Real = $\hat{\theta}$ and Reference θ^d).

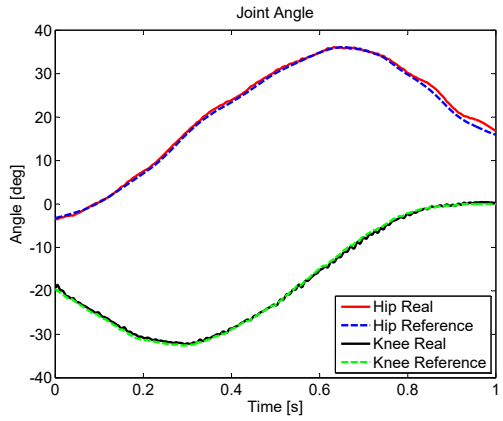

Source: Image generated by the author

Figure 45 – Tracking error. RMS error: 0.51° for hip and 0.40° for knee.

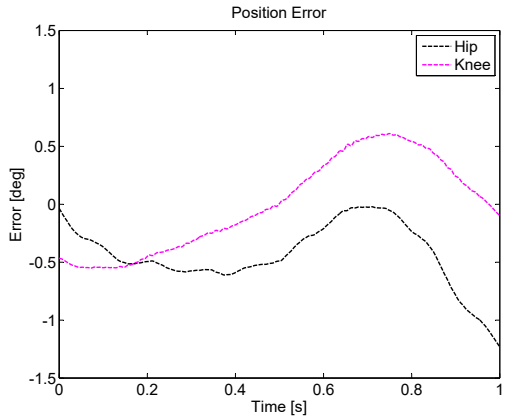

Source: Image generated by the author

Figure 46 shows the torques involved with the movement of the hip. It is possible to observe that in this graph there is no torque of the robot, since the ExoTao has actuators only on the knee, with the other joints being passive with relation to the user. It possible to verify that the PID torque (τ_{PID}) has a reasonably small amplitude when compared to the feedforward torque (τ_{FF}), so it can be concluded that the user torque estimated by the Inverse Dynamics Tool from OpenSim has a reasonable degree of reliability.

Analyzing Figure 47, it is observed that, even with the application of the robot torque to the knee joint, the PID torque was low, compared to the feedforward torque, confirming the fact that the estimated torque is close to the torque actually developed by the subject at the time of the experiment. In the graphs, the blue curves are the total torque of the user and the black curves are the estimated torque, it turns out that they are reasonably close, because of the good estimate provided by the Inverse Dynamics Tool.

Figure 46 – Hip torque. τ_{User} is the user total torque ($\tau_{FF} + \tau_{PID}$).

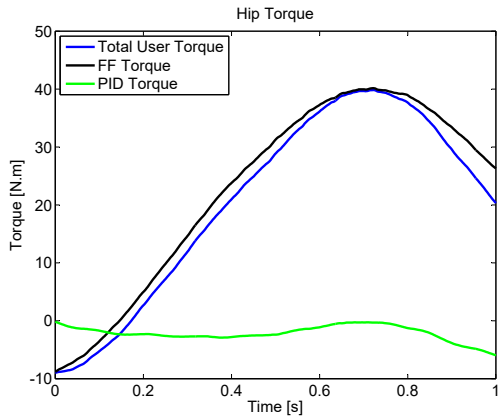

Source: Image generated by the author

Figure 47 – Knee torque. τ_{User} is the user total torque ($\tau_{FF} + \tau_{PID}$).

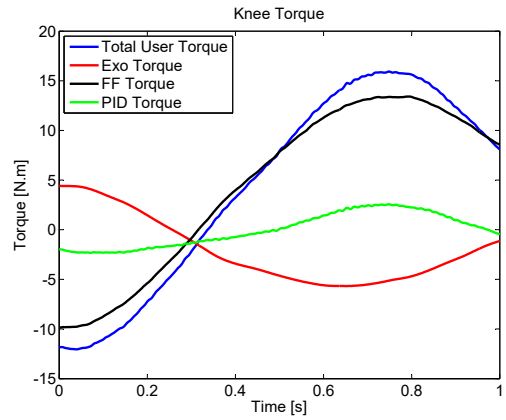

Source: Image generated by the author

4.5.2 Stage 2: Validating the system

In this stage, no adjustments were made to either the model or the simulation algorithm, however new torque inputs and position reference were applied, hoping that the model would perform the movement as well as it did in the previous stage. The stiffness of the impedance control of the ExoTao ((4.6)) was changed to $K_{exo} = 60$. The user continued walking on the treadmill at a speed of 2 km/h.

Figure 48 – Joint position after adjusts. (Real = $\hat{\theta}$ and Reference θ^d).

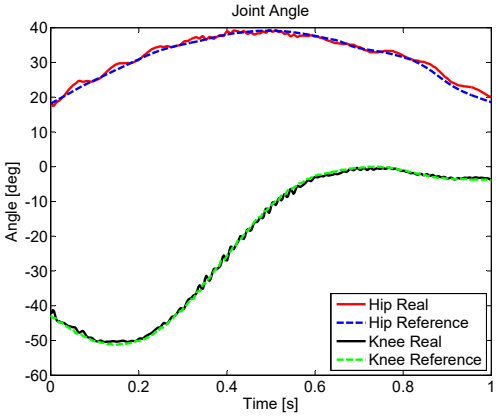

Source: Image generated by the author

Figure 49 – Tracking error. RMS error: 0.57° for hip and 0.48° for knee.

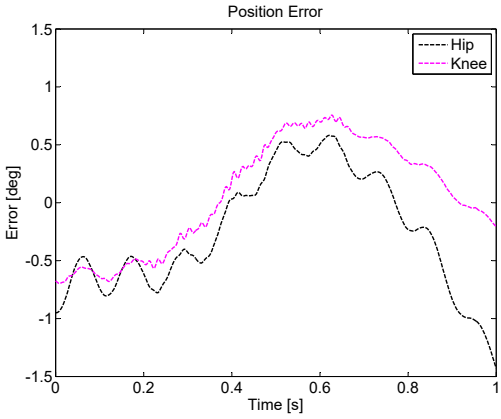

Source: Image generated by the author

Analyzing Figure 48, it is possible to state that the model performed the movement well, proving that, after calibrated and adjusted, the system can reproduce the torques and movements well for a given user wearing the ExoTao directed by an interaction control. In this phase, the maximum position errors were 1.42° for the hip and 0.75° for the knee.

In both stages 1 and 2, the movement analyzed is that of the one-step swing phase, in the act of walking, thus obviously the movements, even they were performed at different times and conditions (different values of K_R for the control of impedance), are similar, as can be seen when comparing Figures 44 and 48.

The torque provided by the robot also does not suffer great variations between phases 1 and 2 (red curves in Figures 47 and 51), since the user is a healthy subject, able to perform the movement by himself, since the exoskeleton uses the interaction torque only to correct small position deviations.

The estimated user torque is also close in both phases, as expected, and in stage 2, despite being slightly more present than in stage 1, the PID torque continues to be significantly lower than the estimated torque, further proof that both the interaction model and the simulation algorithm are feasible and useful.

Figure 50 – Hip torque. τ_{User} is the user total torque ($\tau_{FF} + \tau_{PID}$).

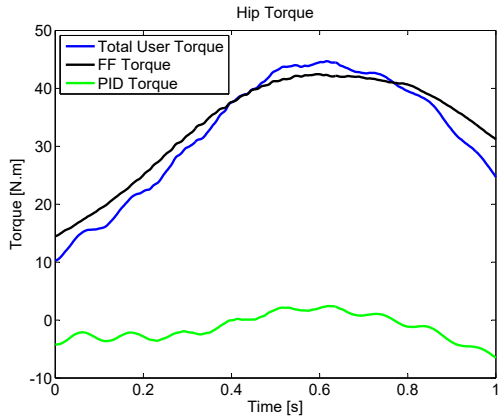

Source: Image generated by the author

Figure 51 – Knee torque. τ_{User} is the user total torque ($\tau_{FF} + \tau_{PID}$).

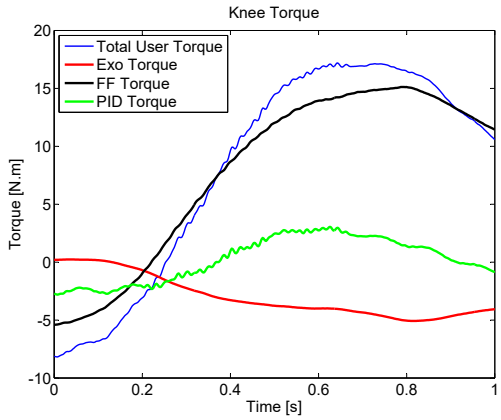

Source: Image generated by the author

With the execution of these two stages, it can be concluded that the model is valid to simulate interaction controls with respect to the swing phase of walking.

4.5.3 Stage 3: Simulating an impedance control

In this stage only the position measured from the ExoTao was used: the robot torque comes from an impedance control stated in the simulation algorithm, as can be seen in the Figure 52. The purpose of this stage is to use an interaction model fitted to an specific user to develop and tune an interaction control. The stiffness of the impedance control was $K = 65$.

Figure 52 – Forward Dynamics Based algorithm to simulation the interaction controls applied to the human-exoskeleton interaction model.

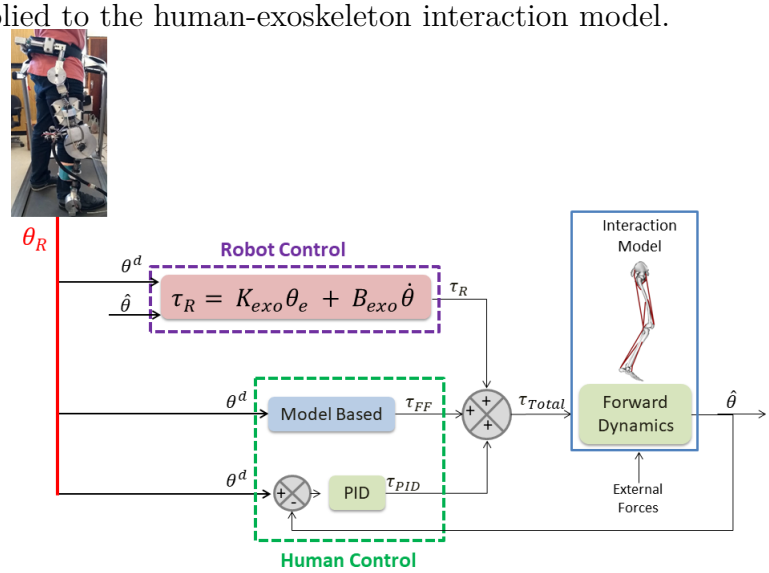

Source: Image generated by the author

In this case, both the hip and ankle joints have robotic actuators, so that the

interaction model was simulated as using the exoskeleton acting on two joints, different from the other tests where the robot acted only on the knee joint.

The model was simulated as the user having some weakness. For this, the torque provided by the feedforward loop (Inverse Dynamics Tool from OpenSim) was decreased in 20%.

Figure 53 – Joint position after adjusts. (Real = $\hat{\theta}$ and Reference θ^d).

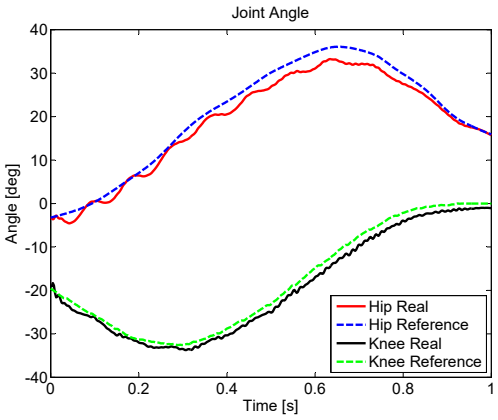

Source: Image generated by the author

Figure 54 – Tracking error. RMS error: 0.51° for hip and 0.39° for knee.

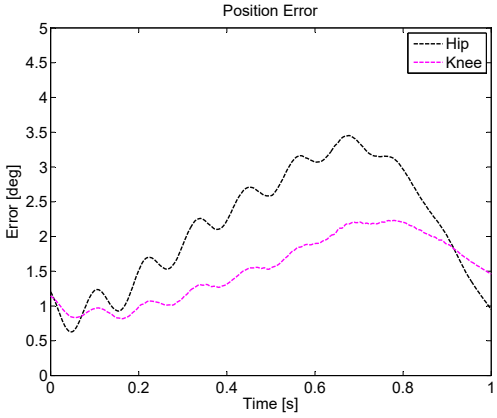

Source: Image generated by the author

Analyzing the Figures 53 and 54, is possible to verify that the model tracked well the reference, with an maximum error less than 3.5° for the hip and 2.5° for the knee.

Figure 55 – Hip torque. τ_{User} is the user total torque ($\tau_{FF} + \tau_{PID}$).

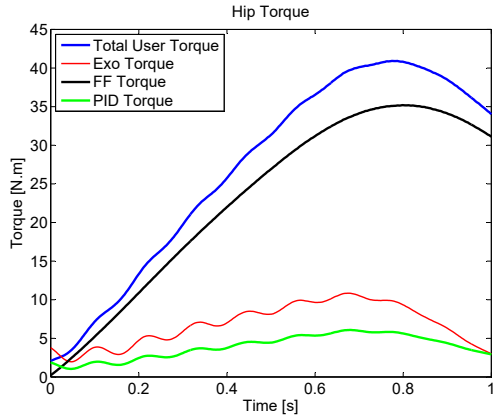

Source: Image generated by the author

Figure 56 – Knee torque. τ_{User} is the user total torque ($\tau_{FF} + \tau_{PID}$).

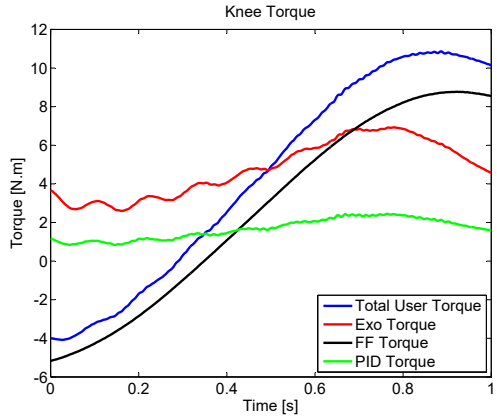

Source: Image generated by the author

Analyzing the Figures 55 and 56, is possible verify that the impedance control

reacted according to the position error, helping the user to accomplish the movement with a minor deviation from the desired position.

Its possible to conclude that the model is feasible and useful to simulate and develop interaction controls in a flexible and reasonably quickly manner. Each simulation took around 10 minutes to be prepared and 8 minutes to be executed, so that, in a total time of approximately one hour, all the simulations presented above were prepared and executed.

5 CONCLUSION

The results obtained with the validation and the simulated controls proved that both the interaction model and the simulation environment are feasible and useful for the development and testing of the interaction controls used in the rehabilitation of lower limbs.

The advantages of using computational interaction models are: agility and flexibility in the development of interaction controls, saving financial resources, time, space and ensuring the safety of both the user and the equipment.

As disadvantages we can mention the limitations regarding the uncertainties of the model, errors of numerical integration, inability to deal with a large number of variables (especially variables with high modeling complexity).

Although there are limitations, this work produced a tool that opens doors for several researches related to robotic neurorehabilitation, such as: development and simulation of interaction controls, modeling of human behavior (by replacing the inverse dynamics and PID in human controls), development and simulation of other types of interaction models and study of the influence of external forces on certain models and controls.

5.1 Next Works

For future work, it is suggested that a model optimization routine be included, in order to reduce the degree of uncertainty of the model in relation to a specific subject. It is also suggested that the integration algorithm based on forward dynamics is improved in order to be able to simulate not only the swing phase during gait, but a complete step, including stance phase and the ground reaction forces.

BIBLIOGRAPHY

AGARWAL, P.; NEPTUNE, R. R.; DESHPANDE, A. D. A simulation framework for virtual prototyping of robotic exoskeletons. **Journal of Biomechanical Engineering**, ASME International, v. 138, n. 6, p. 1–15, 2016.

AL., A. R. et. **Royal College of Physicians of London: National clinical guidelines for stroke**. 2. ed. London, England: The Lavenham Press Ltd, 2004. ISBN 1-86016-208-8.

BALABAN, P. M. et al. Central pattern generators. **Neuroscience and Behavioral Physiology**, v. 45, n. 1, p. 42–57, 2015. ISSN 1573-899X.

BAYON, C. et al. Performance-based adaptive assistance for diverse subtasks of walking in a robotic gait trainer: Description of a new controller and preliminary results. In: **2018 7th IEEE International Conference on Biomedical Robotics and Biomechatronics (Biorob)**. Enschede, The Netherlands: [s.n.], 2018. p. 414–419.

BRAININ, M.; HEISS, W. D. **Textbook of stroke medicine**. Cambridge, England: Cambridge University Press, 2009. ISBN 978-0-511-69119-5.

CAPLAN, L. R. **Stroke**. New York, USA: American Academy of Neurology Press, 2005. ISBN 1-932603-14-X.

DELP, S. L. et al. Opensim: Open-source software to create and analyze dynamic simulations of movement. **IEEE Transactions on Biomedical Engineering**, v. 54, n. 11, p. 1940–1950, 2007.

DEMBIA, C. **Dynamic Walker Example**. 2014. Disponível em: <https://github.com/opensim-org/opensim-core/tree/661433ec8f0778b85768b451a3714488224c419e/OpenSim/Wrapping/Java/Matlab/Dynamic_Walker_Example>.

DIAZ, I.; GIL, J. J.; SANCHEZ, E. Lower-limb robotic rehabilitation: Literature review and challenges. **Journal of Robotics**, v. 2011, p. 1–11, 2011.

DIETZ, V.; NEF, T.; RYMER, W. Z. **Neurorehabilitation Technoloby**. Chicago, USA: Springer, 2012. ISBN 978-1-4471-2277-7.

DURANDAU, G. et al. Emg-driven models of human-machine interaction in individuals wearing the h2 exoskeleton. **IFAC-PapersOnLine**, v. 49, p. 200–203, 2016.

ETHIER, C. R.; SIMMONS, C. A. **Introductory Biomechanics From Cells to Organisms**. Cambridge, England: Cambridge University Press, 2017. ISBN 978-0-511-27360-5.

FREY, S. H. et al. Neurological principles and rehabilitation of action disorders. **Neurorehabilitation and Neural Repair**, SAGE Publications, v. 25, n. 5, p. 6–20, 2011.

GHANNADI, B. et al. Nonlinear model predictive control of an upper extremity rehabilitation robot using a two-dimensional human-robot interaction model. In: **2017 IEEE/RSJ International Conference on Intelligent Robots and Systems (IROS)**. Vancouver, Canada: [s.n.], 2017. p. 502–507.

GUZMÁN, C. H. et al. Robust control of a hip–joint rehabilitation robot. **Biomedical Signal Processing and Control**, Elsevier BV, v. 35, p. 100–109, 2017.

HALL, J. E. **Guyton and Hall textbook of medical physiology**. 13. ed. Philadelphia, USA: Elsevier, 2017. ISBN 978-1-4557-7005-2.

HANDFORD, M. L.; SRINIVASAN, M. Robotic lower limb prosthesis design through simultaneous computer optimizations of human and prosthesis costs. **Scientific Reports**, Springer Nature, v. 6, n. 1, feb 2016.

_____. Energy-optimal human walking with feedback-controlled robotic prostheses: A computational study. **IEEE Transactions on Neural Systems and Rehabilitation Engineering**, Institute of Electrical and Electronics Engineers (IEEE), v. 26, n. 9, p. 1773–1782, sep 2018.

HOGAN, N. Robot-aided neuro-recovery. **ASME. Mechanical Engineering**, v. 136, n. 9, p. 3–5, 2014.

IBARRA, J. C. P. **Controle de Impedância Adaptativo aplicado à Reabilitação Robótica do Tornozelo**. 2014. Dissertação (mathesis), São Carlos, Brazil, 2014.

JUTINICO, A. L. et al. Markovian robust compliance control based on electromyographic signals. In: **2018 7th IEEE International Conference on Biomedical Robotics and Biomechatronics (Biorob)**. Enschede, The Netherlands: [s.n.], 2018.

_____. Impedance control for robotic rehabilitation: A robust markovian approach. **Frontiers in Neurorobotics**, v. 11, p. 43, 2017. ISSN 1662-5218.

KHAMAR, M.; EDRISI, M. Designing a backstepping sliding mode controller for an assistant human knee exoskeleton based on nonlinear disturbance observer. **Mechatronics**, v. 54, p. 121–132, 2018.

KIM, J.; KIM, J. An impedance control of human ankle joint using functional electrical stimulation. In: **2018 7th IEEE International Conference on Biomedical Robotics and Biomechatronics (Biorob)**. Enschede, The Netherlands: [s.n.], 2018. p. 1230–1235.

KIRTLEY, C. **Clinical Gait Analysis: Theory and Practice**. London, England: Churchill Livingstone, 2006. ISBN 0443100098.

KREBS, H. I. et al. Rehabilitation robotics: performance-based progressive robot-assisted therapy. **Autonomous Robots**, v. 15, n. 1, p. 7–20, 2003.

LAM, T.; ANDERSCHITZ, M.; DIETZ, V. Contribution of feedback and feedforward strategies to locomotor adaptations. **Journal of Neurophysiology**, American Physiological Society, v. 95, n. 2, p. 766–773, 2006.

LAPRE, A. K.; UMBERGER, B. R.; SUP, F. Simulation of a powered ankle prosthesis with dynamic joint alignment. In: **2014 36th Annual International Conference of the IEEE Engineering in Medicine and Biology Society**. Chicago, USA: IEEE, 2014.

LUM, P. S. et al. Robot-assisted movement training compared with conventional therapy techniques for the rehabilitation of upper-limb motor function after stroke. **Archives of Physical Medicine and Rehabilitation**, v. 83, p. 952–959, 2002.

MACKAY, J.; MENSAH, G. A. **The Atlas of Heart Disease and Stroke**. Switzerland: World Health Organization, 2004. ISBN 9789241564373.

MANSOURI, M.; REINBOLT, J. A. A platform for dynamic simulation and control of movement based on OpenSim and MATLAB. **Journal of Biomechanics**, Elsevier BV, v. 45, n. 8, p. 1517–1521, 2012.

MARLER, J. R. **Stroke for Dummies**. Indianapolis, USA: Wiley Publishing, 2005. ISBN 0-7645-7201-6.

MOSCONI, D. et al. Human-exoskeleton interaction model applied to robotic neurorehabilitation of lower limbs. In: **25th ABCM International Congress of Mechanical Engineering**. Uberlandia, Brazil: ABCM, 2019.

MOSCONI, D.; NUNES, P. F.; SIQUEIRA, A. A. G. Human-exoskeleton computational model: an approach to the human-machine interaction problem in robotic assisted therapy. In: **IV Simpósio do Programa de Pós-Graduação em Engenharia Mecânica**. São Carlos, Brazil: USP, 2019.

MOSCONI, D.; SIQUEIRA, A. A. G. Simulation of impedance based interaction control for robotic neurorehabilitation using a human-exoskeleton interaction model inspired by the human internal model. In: **XIV CONFERÊNCIA BRASILEIRA DE DINÂMICA, CONTROLE E APLICAÇÕES**. São Carlos, Brazil: ABCM, 2019.

MS. **Ministério da Saúde - AVC: causas, sintomas, tratamentos, diagnóstico e prevenção**. 2018. Disponível em: <http://portalms.saude.gov.br/saude-de-a-z/acidente-vascular-cerebral-avc>.

_____. **Ministério da Saúde - Panorama do AVC no Brasil**. 2018. Disponível em: <https://bit.ly/2s1qzNh>.

MURIE-FERNáNDEZ, M. et al. Neuro-rehabilitation after stroke. **Neurología**, v. 25, p. 189–196, 2010.

NUNES, P. F. et al. Influência de um exoesqueleto sobre as características cinéticas e musculares durante a marcha utilizando primitivas de movimento. In: **Proceedings do 6º Encontro Nacional de Engenharia Biomecânica**. Aguas de Lindoia, Brazil: ABCM, 2018. v. 1, p. 1–6.

NUNES, P. F.; MOSCONI, D.; SIQUEIRA, A. A. G. Control design inspired by primitive motors to coordinate the functioning of an active knee orthosis for robotic rehabilitation. In: **X Congreso Iberoamericano de Tecnologias de Apoyo a la Discapacidad**. Buenos Aires, Argentina: AITADIS, 2019.

NUNES, P. F.; SANTOS, W. M. dos; SIQUEIRA, A. A. G. Control strategy based on kinetic motor primitives for lower limbs exoskeletons. In: **10th IFAC Symposium on Biological and Medical Systems**. São Paulo, Brazil: ElsevierBV, 2018. v. 51, p. 402–406.

PARKER, J. N.; PARKER, P. M. **The official patient's sourcebook on stroke**. San Diego, USA: ICON Health Publications, 2002. ISBN 0-597-83450-4.

PASTORE, A. et al. Motor intention decoding during active and robot-assisted reaching. In: **2018 7th IEEE International Conference on Biomedical Robotics and Biomechatronics (Biorob)**. Enschede, The Netherlands: [s.n.], 2018. p. 312–317.

PEÑA, G. G. **Controle de Impedância Adaptativo Dirigido por EMG para Reabilitação Robótica**. 2017. Tese (phdthesis) — University of São Paulo - São Carlos School of Engineering, São Carlos, Brazil, 2017.

PEÑA, G. G. et al. Feasibility of an optimal emg-driven adaptive impedance control applied to an active knee orthosis. **Robotics and Autonomous Systems**, n. 112, p. 98–108, 2019.

PETERSON, D. R.; BRONZINO, J. D. **Biomechanics Principles and Aplications**. Miami, USA: CRC Press, 2008. ISBN 978-0-8493-8534-6.

PONS, J. L.; TORRICELLI, D. **Emergind Therapies on Neurorehabilitation**. New York, USA: Springer, 2014. v. 4. ISBN 978-3-642-38556-8.

REINKENSMEYER, D. J.; EMKEN, J. L.; CRAMER, S. C. Robotics, motor learning and neurologic recovery. **Annual Review of Biomedical Engineering**, v. 6, p. 497–525, 2004.

RIENER, R. et al. Patient-cooperative strategies for robot-aided treadmill training: First experimental results. **IEEE TRANSACTIONS ON NEURAL SYSTEMS AND REHABILITATION ENGINEERING**, v. 13, n. 3, p. 380–394, 2005.

RUDD, A.; IRWIN, P.; PENHALE, B. **Stroke**. London, England: Class Publishing, 2004. ISBN 1-85959-113-2.

SANTOS, W. M. dos et al. Design and evaluation of a modular lower limb exoskeleton for rehabilitation. In: **2017 International Conference on Rehabilitation Robotics (ICORR)**. London, England: IEEE, 2017.

SELZER, M. E. et al. **Textbook of Neural Repair and Rehabilitation**. Cambridge, England: Cambridge University Press, 2006. ISBN 978-0-511-16919-9.

SINGH, I. **Inderbir Singh's Textbook of Human Neuroanatomy Fundamental and Clinical**. 10. ed. New Delhi, India: The Health Sciences Publisher, 2018. ISBN 978-93-5270-148-3.

SOUSA, A. C. C. de; FREIRE, J. P. C. D.; BO, A. P. L. Integrating hip exosuit and FES for lower limb rehabilitation in a simulation environment. **IFAC-PapersOnLine**, Elsevier BV, v. 51, n. 34, p. 302–307, 2019.

SOUSA, A. C. C. de et al. A comparative study on control strategies for fes cycling using a detailed musculoskeletal model. **IFAC-PapersOnline**, v. 49, n. 32, p. 204–209, 2016.

VUKOBRATOVIC, M. et al. **Biped Locomotion: Dynamics, Stability, Control and Application**. Berlin, Germany: Springer-Verlag, 1990. ISBN 978-3-642-83008-2.

WHO. **World Health Organization - Gloabal Atlas on cardiovascular disease prevention and control**. Switzerland: World Health Organization, 2011. ISBN 978-92-4-156437-3.

_____. Report, **World Health Organization - World Report on Disability**. 2011. Disponível em: <http://www.who.int/disabilities/world_report/2011/report.pdf>.

_____. Report, **World Health Organization - The top 10 causes of death**. 2018. Disponível em: <http://www.who.int/news-room/fact-sheets/detail/the-top-10-causes-of-death>.

WOLPERT, D. M.; MIALL, R. C.; KAWATO, M. Internal models in the cerebellum. **Trends in Cognitive Sciences**, v. 2, n. 9, p. 338–347, 1998.

WYART, C. Taking a big step towards understanding locomotion. **Trends in Neurosciences**, v. 41, n. 12, p. 869–870, 2018. ISSN 0166-2236.


EESC • USP